

Multiwavelength view of halos around pulsars

Mattia Di Mauro



F. Donato and S. Manconi

**First halo around pulsar workshop
December 3 2020.**

Overview of the talk

1. *Detection of a γ -ray halo around Geminga with the Fermi-LAT data and implications for the positron flux* MDM, S. Manconi, F. Donato, PRD 100, 123015 (2019)
2. *Evidences of low-diffusion bubbles around Galactic pulsars* MDM, S. Manconi, F. Donato PRD 101, 103035 2020
3. *Prospects for the detection of synchrotron halos around middle-age pulsars* MDM, S. Manconi, F. Donato Astro2020

- **Inverse Compton Scattering (ICS) halos (gamma rays)**

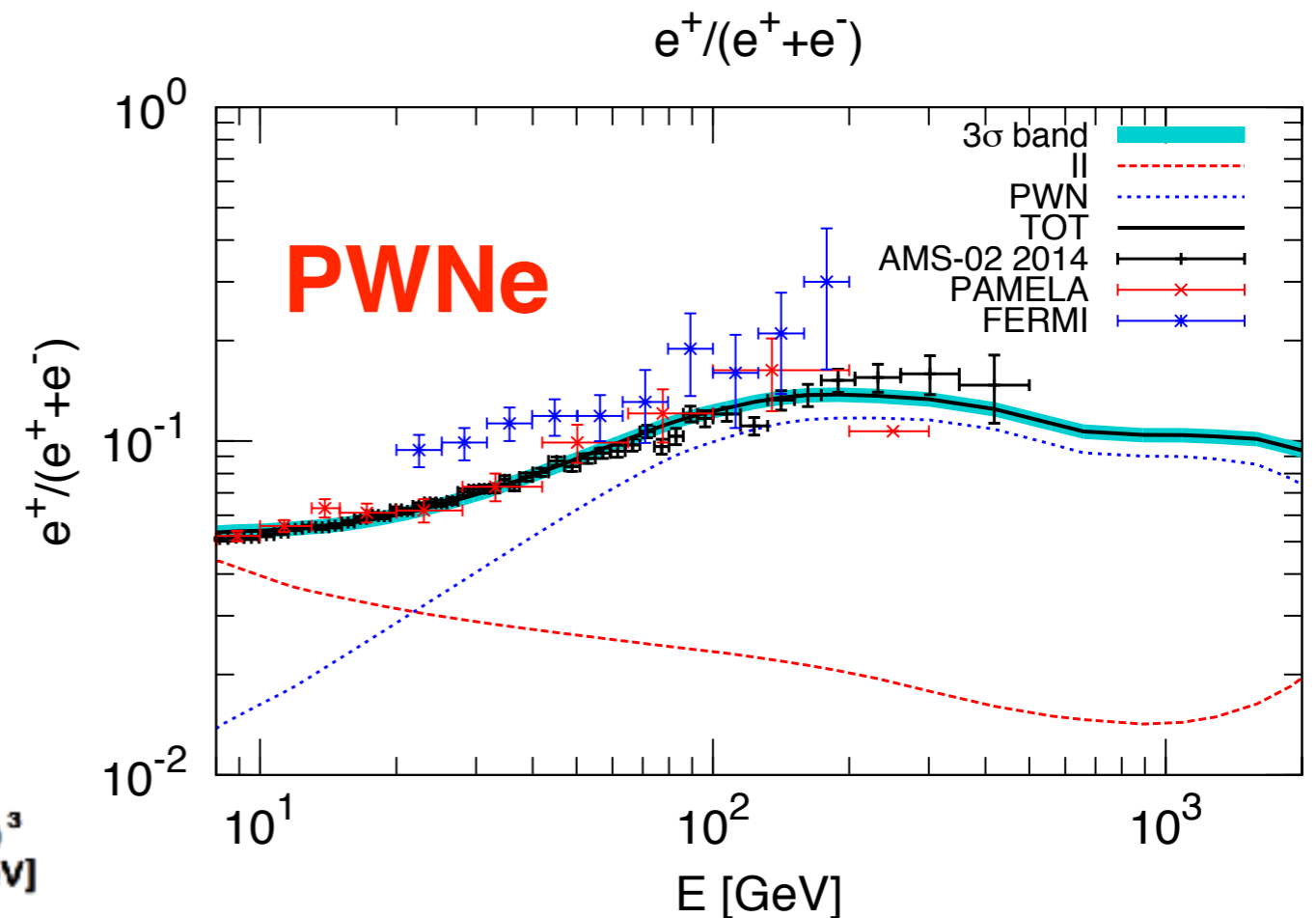
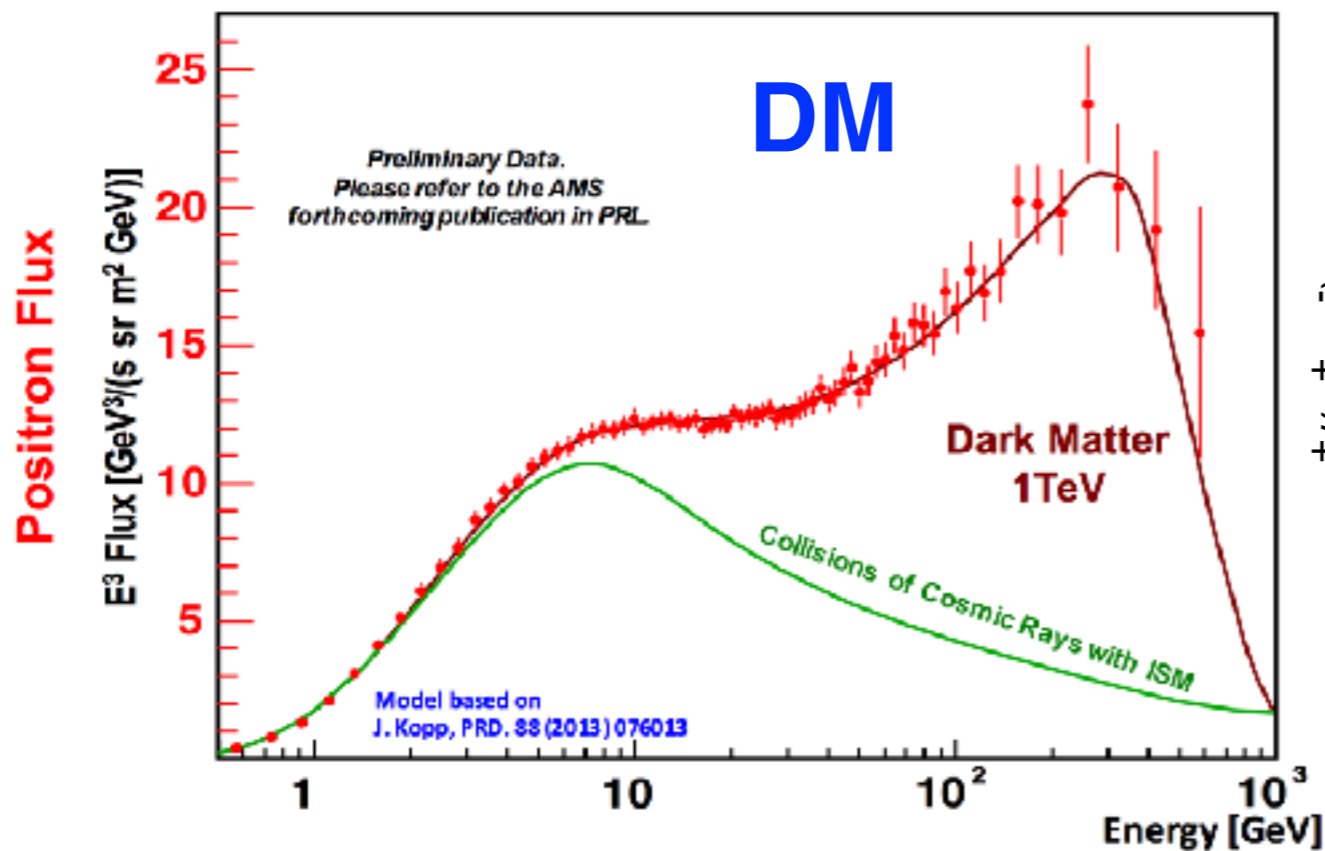
- Angular extension at GeV and TeV.
- Proper motion effect.
- Constraining the positron excess.
- Current results on ICS halos at GeV and TeV energies.

- **Synchrotron halos (from radio to X rays)**

- Angular extension at radio and X-ray energies.
- Current limitations for current X-ray and radio observations.
- Prospects for detection by current and future experiments.

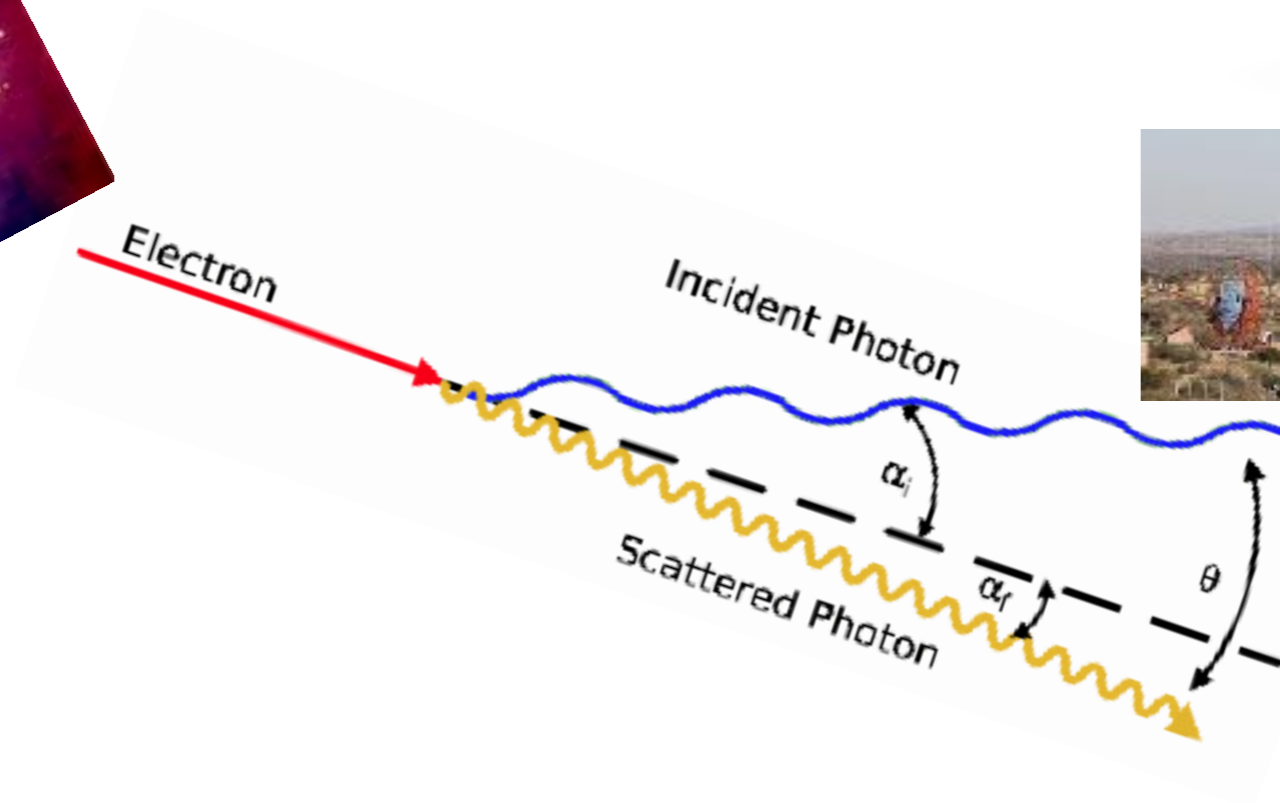
Origin of cosmic-ray positrons

- Positrons are emitted through the secondary mechanism (CRs ISM \rightarrow X e^+).
- An excess of positrons above 10 GeV with respect to the secondary production has been measured by different experiments.
- Annihilation or decay of dark matter particles and emission from PWNe have been suggested as possible interpretations.



(M. Di Mauro and others. JCAP 1605 (2016) no.05, 031., M. Di Mauro and others. JCAP 04 (2014) 006.)

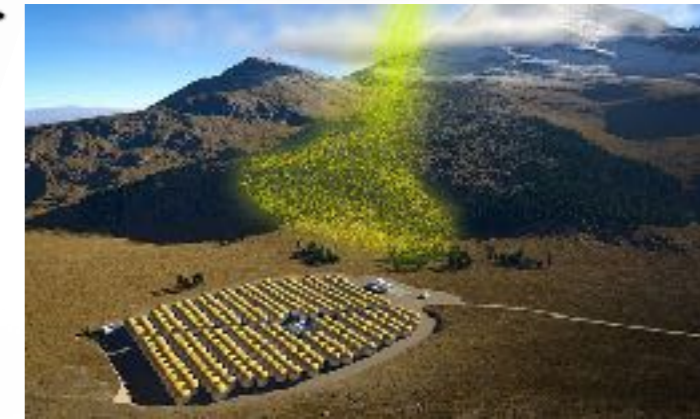
γ rays produced by inverse Compton scattering (ICS)



IACTs



HAWC

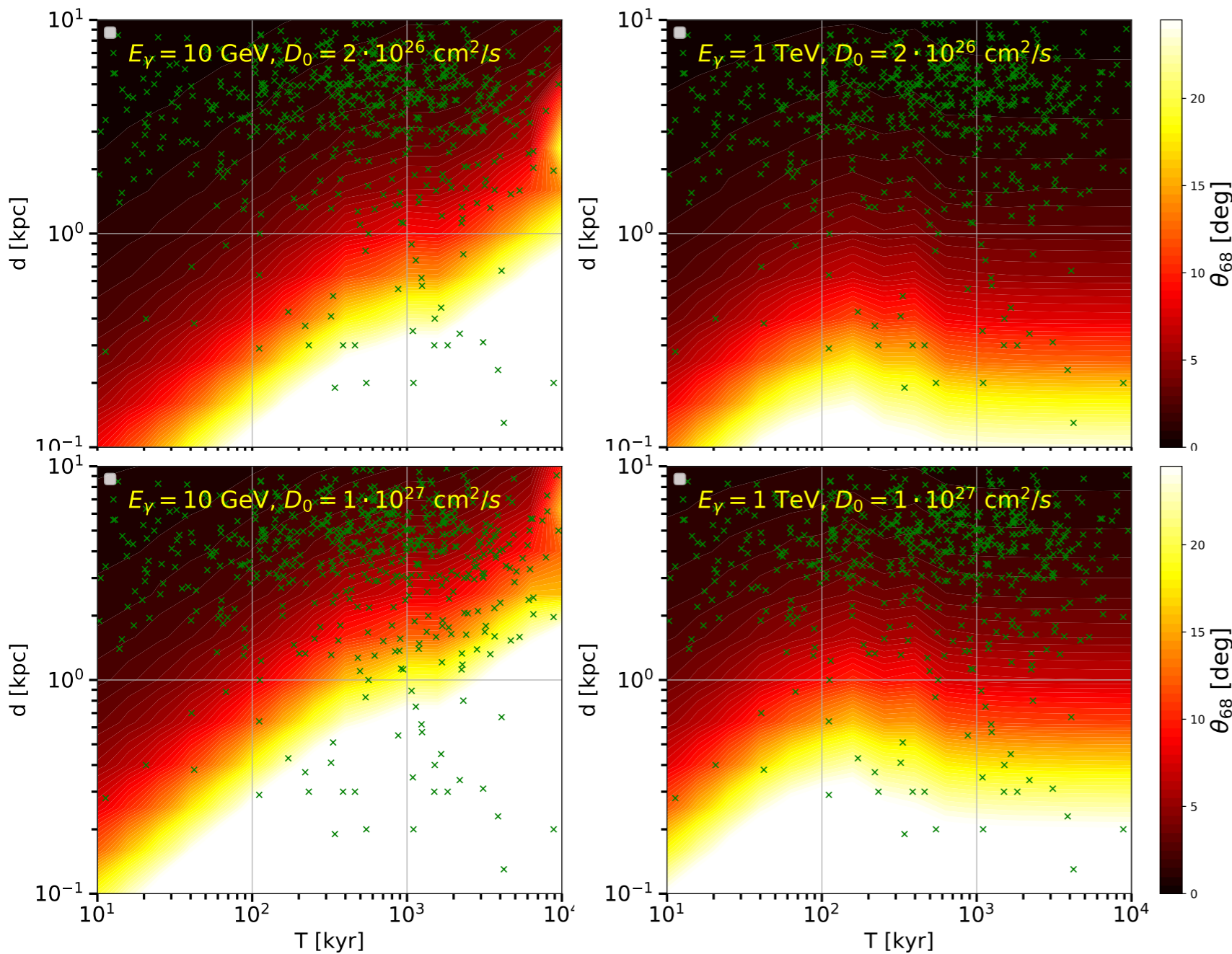


Fermi-LAT



ICS halo extension

$$\Phi_{\gamma}^{68\%} = 2\pi \int_0^{\theta_{\text{EXT}}} \frac{d\Phi_{\gamma}}{d\theta} \sin \theta d\theta$$

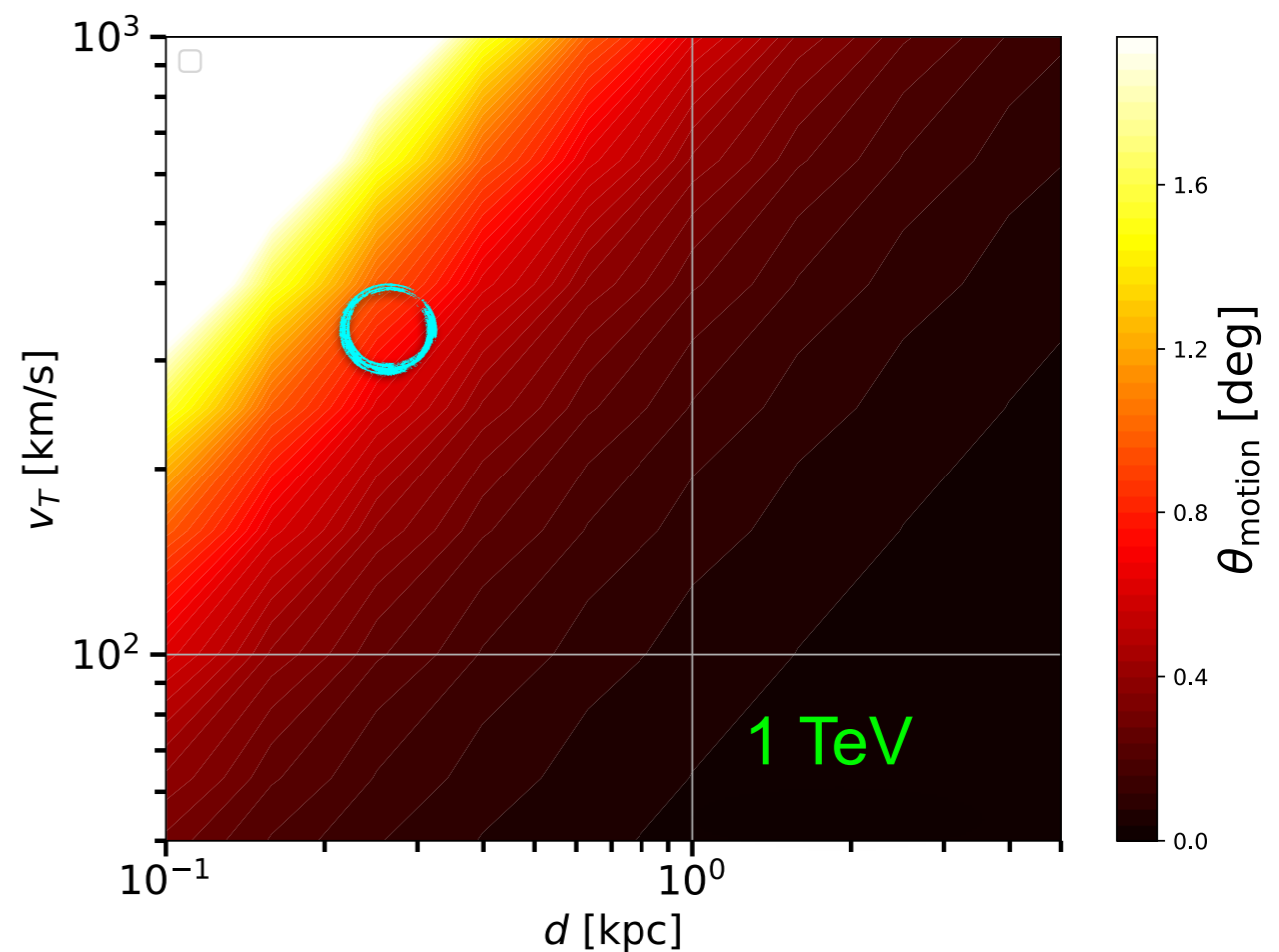
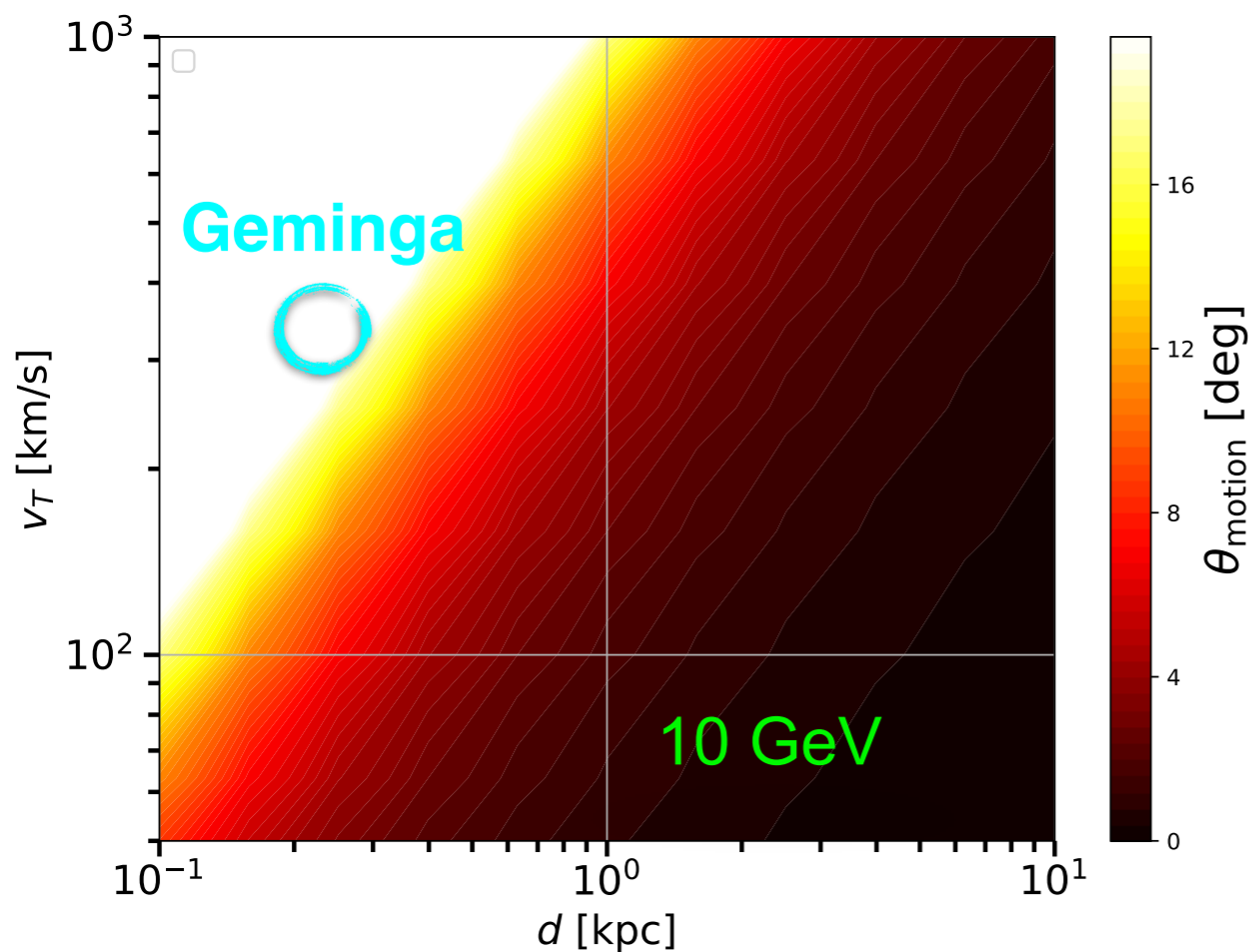


x ATNF catalog pulsars

- $D > 10^{27} \text{ cm}^2/\text{s}$ \rightarrow several ICS halos undetectable by IACTs and HAWC.
- At GeV most of the pulsars have a very extended halo.

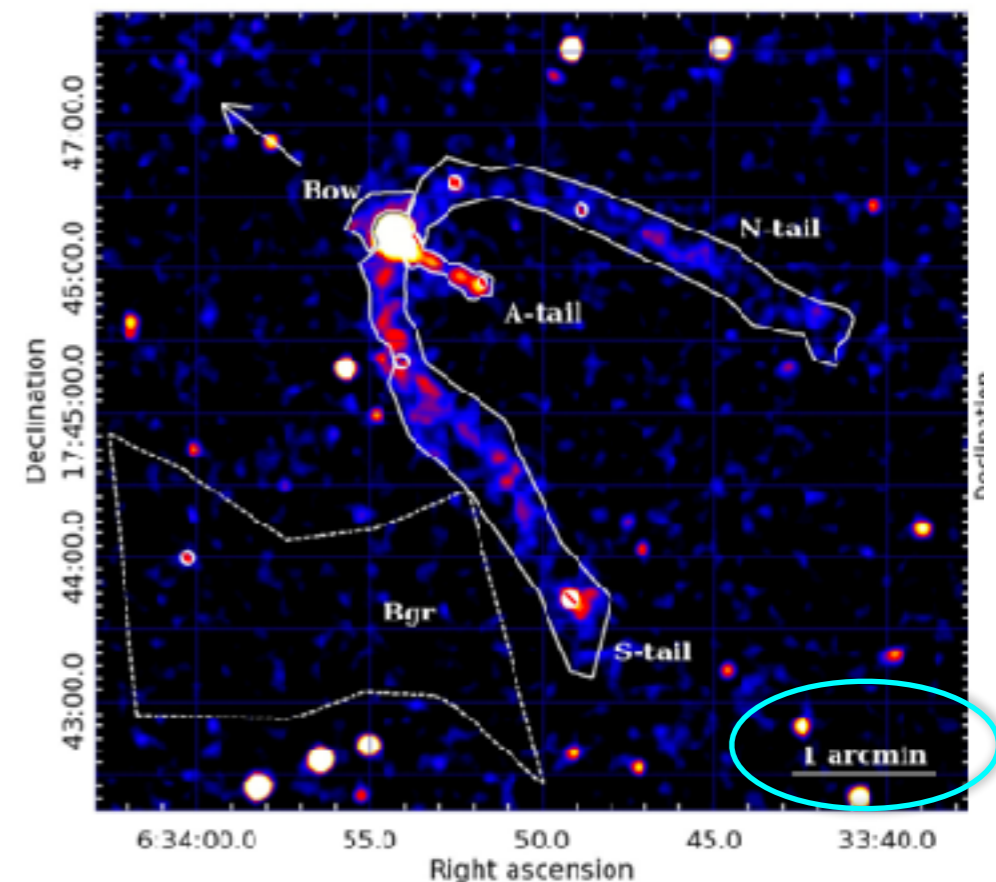
Pulsar proper motion

- The average pulsar proper motion is around 200 km/s (Faherty et al. 2007).
- At GeV the proper motion is not relevant only for $d > a$ few kpc and $T < a$ few hundreds kyr.
- At TeV the effect is much smaller.

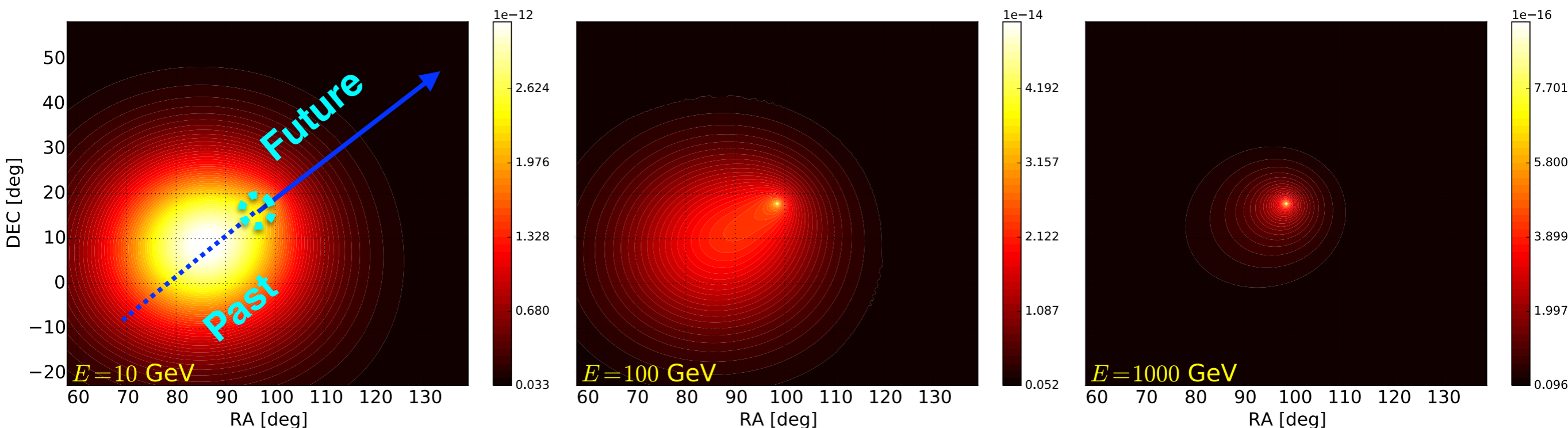


Geminga proper motion

- Geminga has a proper motion of **211 km/s** which implies this pulsar moved about **70 pc** across its age.
- We have implemented this effect in our model.
- Our analysis is unique in γ -ray astronomy because we search for a source that is moving across the sky in γ rays.

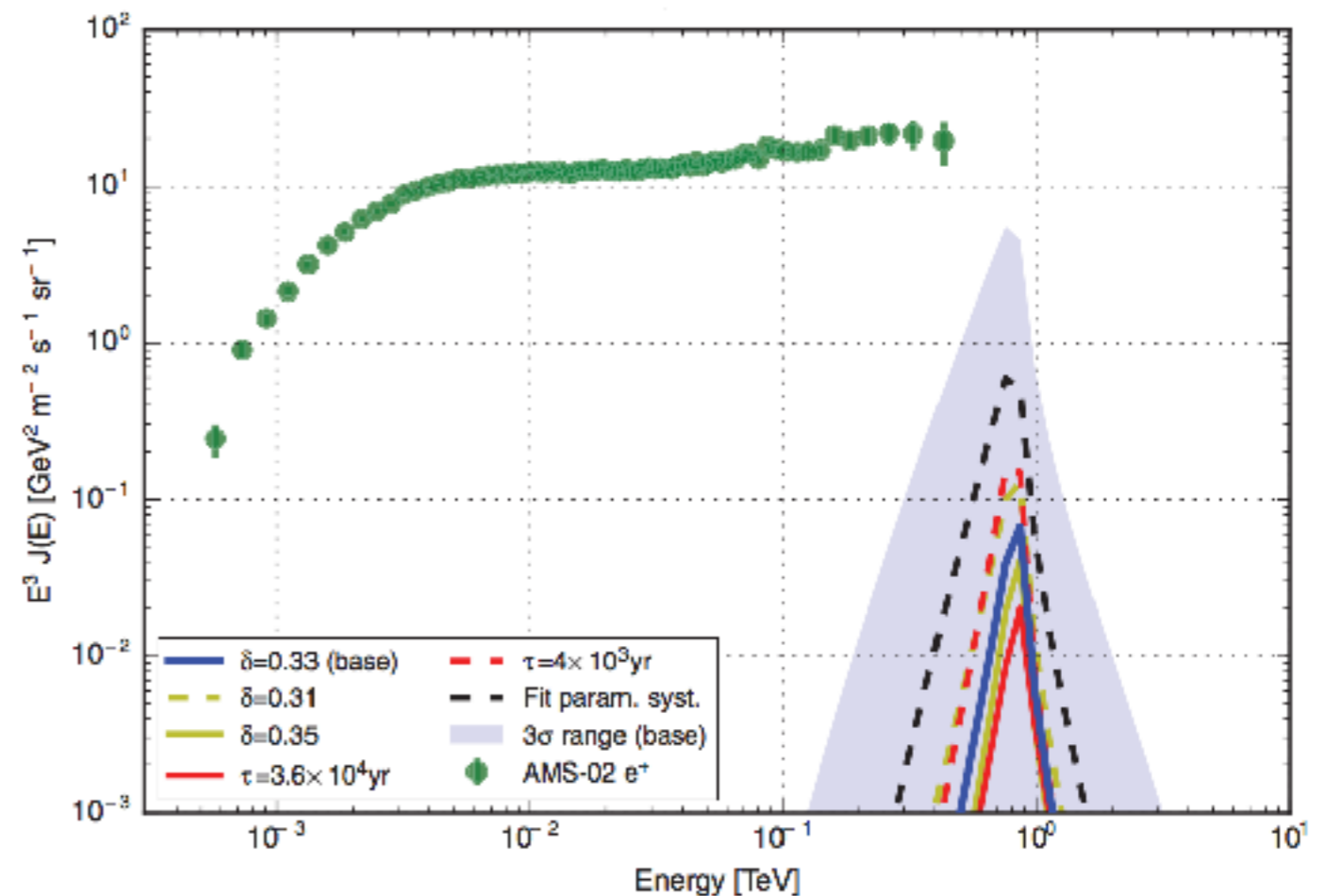
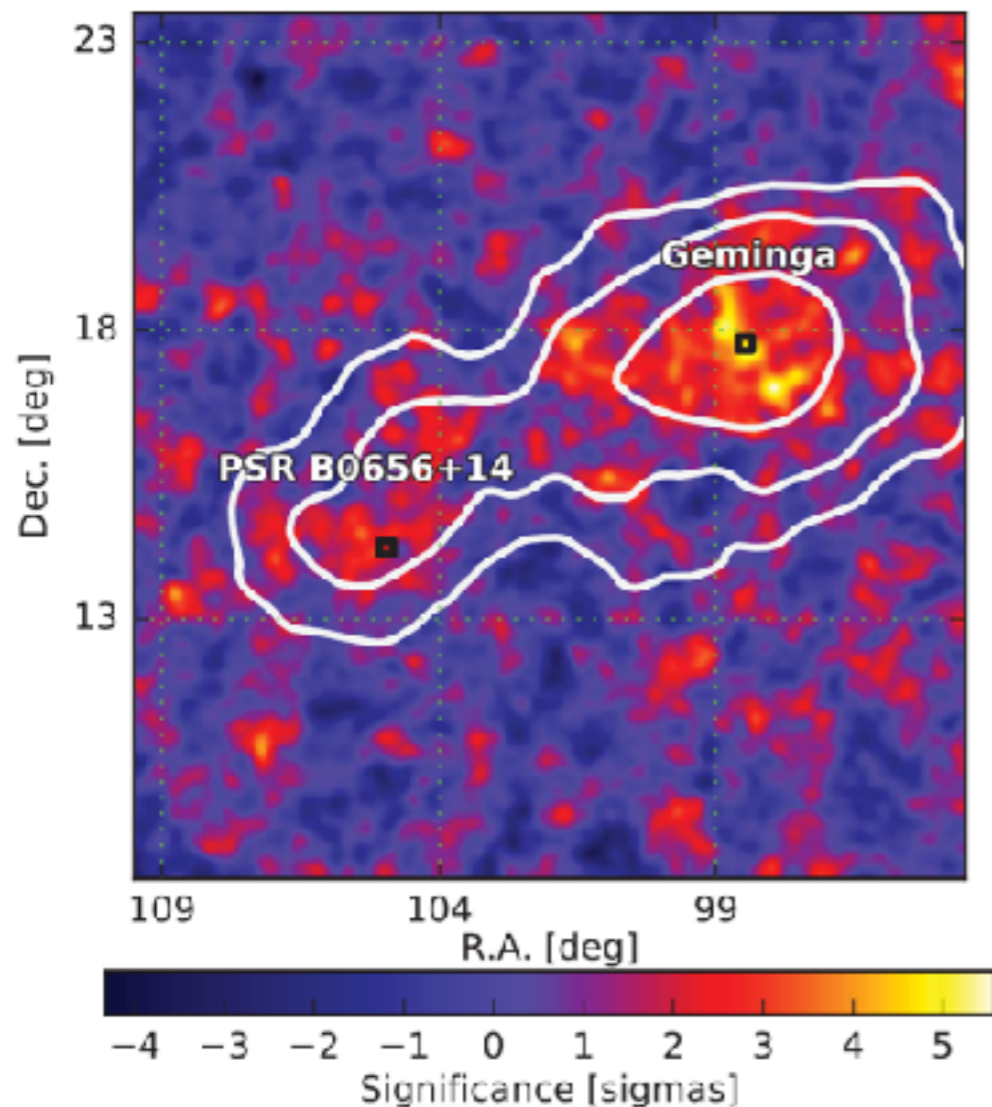


Posselt et al. 2008



HAWC results for Geminga and Monogem PWNe

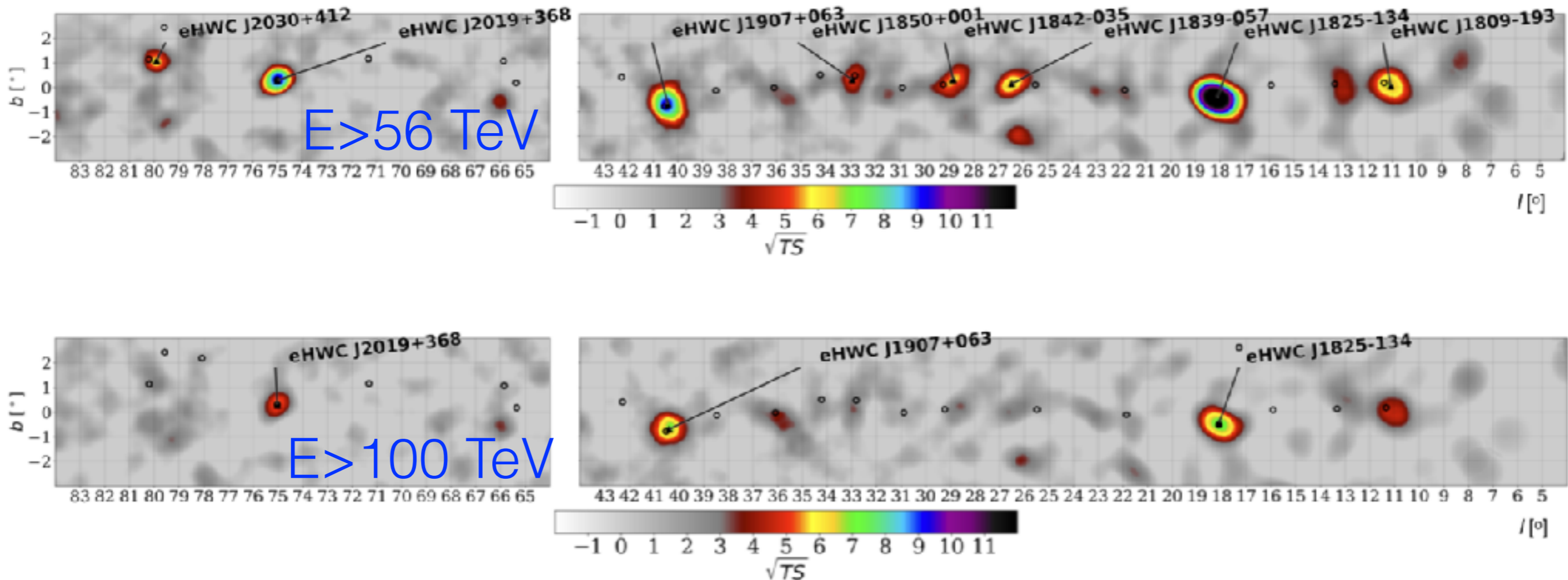
- HAWC detected an extended emission from Geminga and Monogem PWNe for $E > 5$ TeV.
- Interpreted as ICS emission from e^+ and e^- accelerated from the PWN.
- **In the vicinity of the PWN, the diffusion coefficient D must be about 500 times smaller than the average in the Galaxy.**



Recent results from HAWC

A New Population of Ultra-High-Energy Gamma-Ray Sources Detected by HAWC

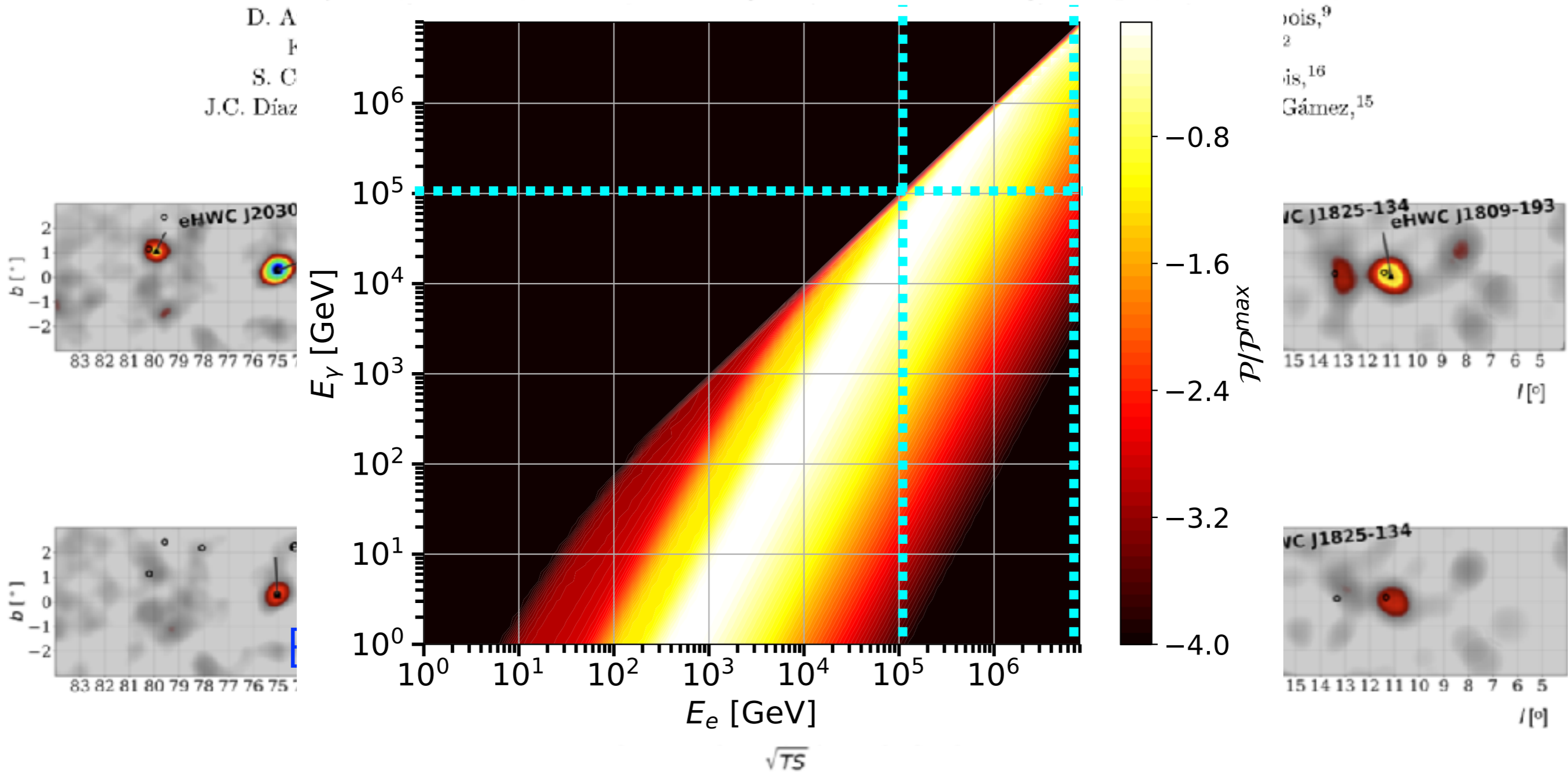
A.U. Abeysekara,¹ A. Albert,² R. Alfaro,³ J.R. Angeles Camacho,³ J.C. Arteaga-Velázquez,⁴ K.P. Arunbabu,⁵
D. Avila Rojas,³ H.A. Ayala Solares,⁶ V. Baghmanyan,⁷ E. Belmont-Moreno,³ S.Y. BenZvi,⁸ C. Brisbois,⁹
K.S. Caballero-Mora,¹⁰ T. Capistrán,¹¹ A. Carramiñana,¹¹ S. Casanova,⁷ U. Cotti,⁴ J. Cotzomi,¹²
S. Coutiño de León,¹¹ E. De la Fuente,^{13,14} C. de León,⁴ S. DiChiara,¹⁵ B.L. Dingus,² M.A. DuVernois,¹⁶
J.C. Díaz-Vélez,^{13,14} R.W. Ellsworth,⁹ K. Engel,⁹ C. Espinoza,³ H. Fleischhack,¹⁷ N. Fraija,¹⁵ A. Galván-Gómez,¹⁵



Recent results from HAWC

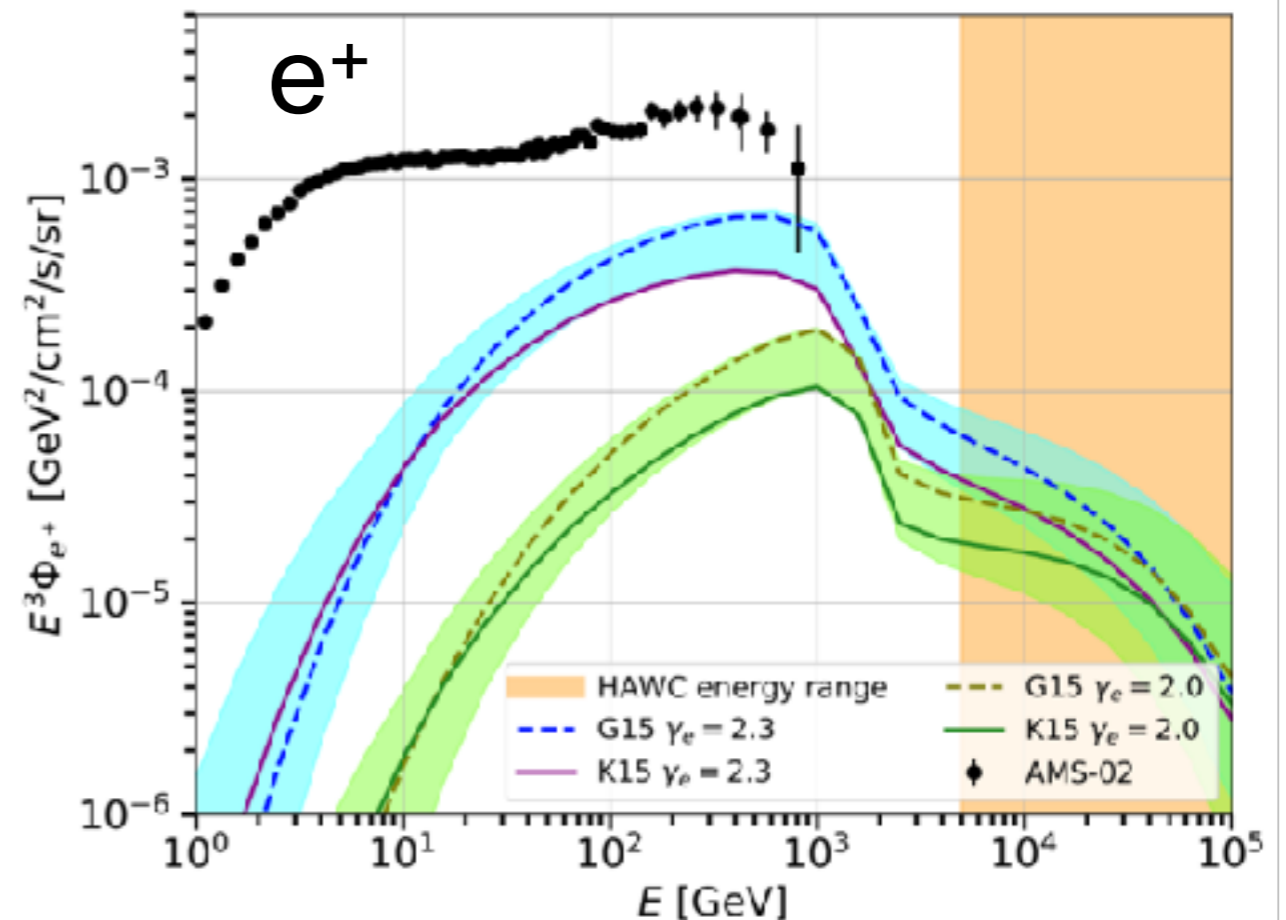
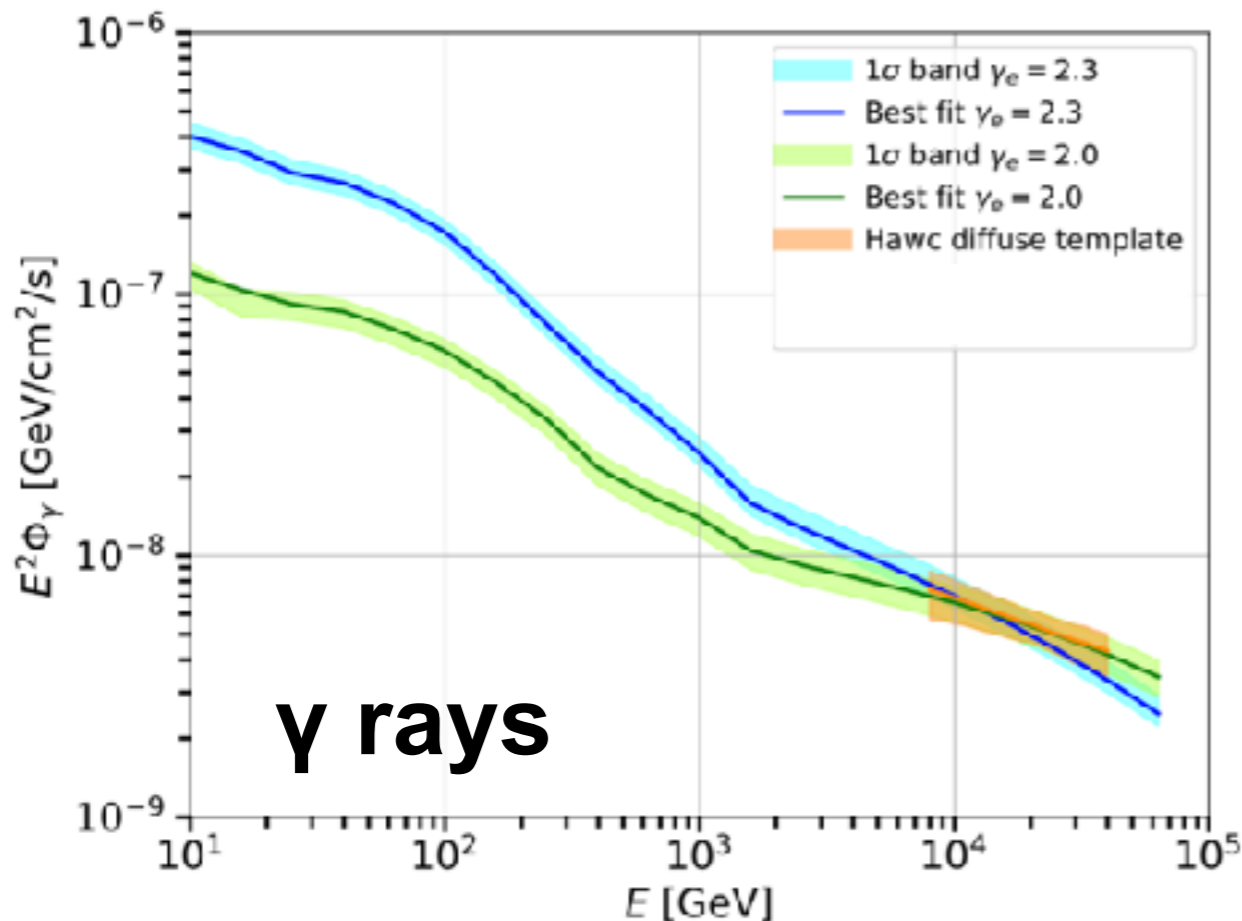
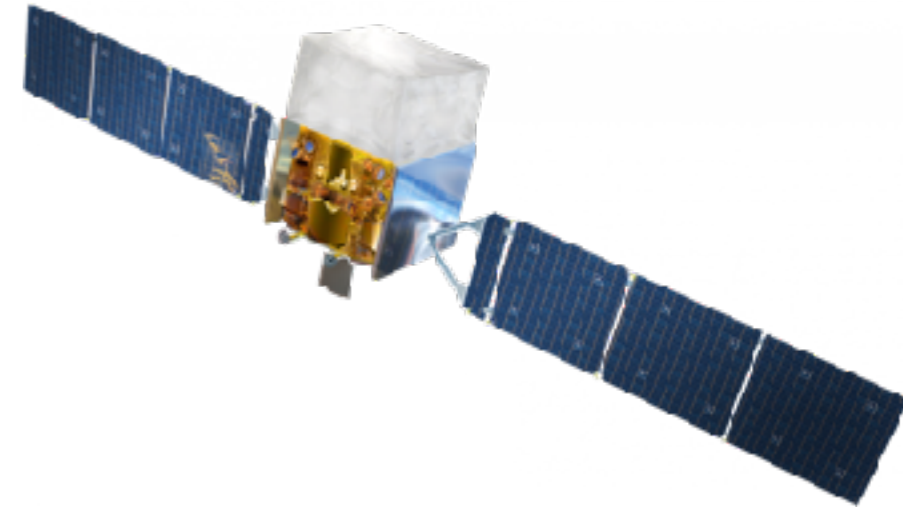
A New Population of Ultra-High-Energy Gamma-Ray Sources Detected by HAWC

A.U. Abeysekera,¹ A. Albert,² R. Alfaro,³ J.R. Angeles Camacho,³ J.C. Arteaga-Velázquez,⁴ K.P. Arunbabu,⁵
 D. A.
 F.
 S. C.
 J.C. Díaz



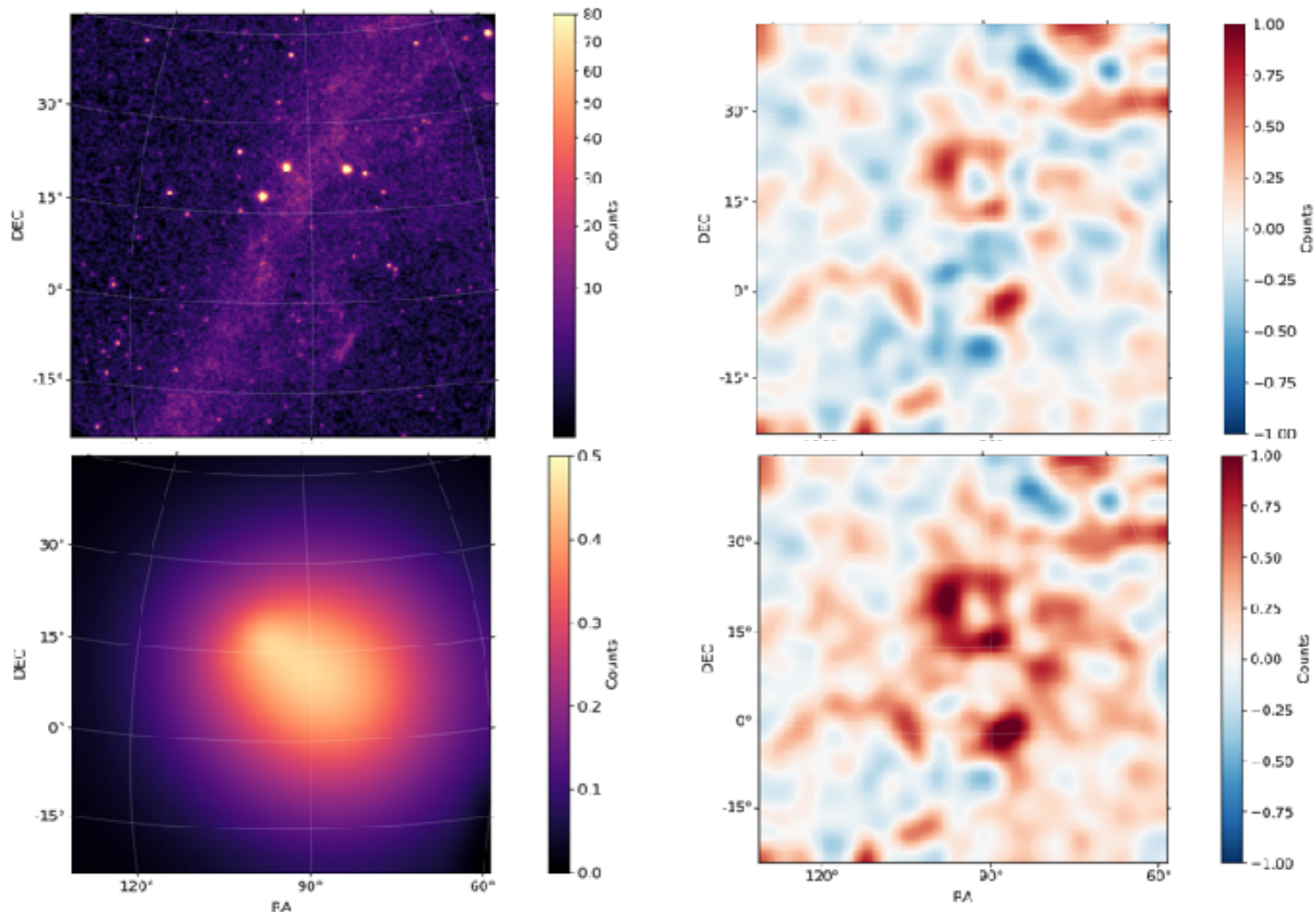
Predictions for the e^+ flux from Geminga using HAWC data

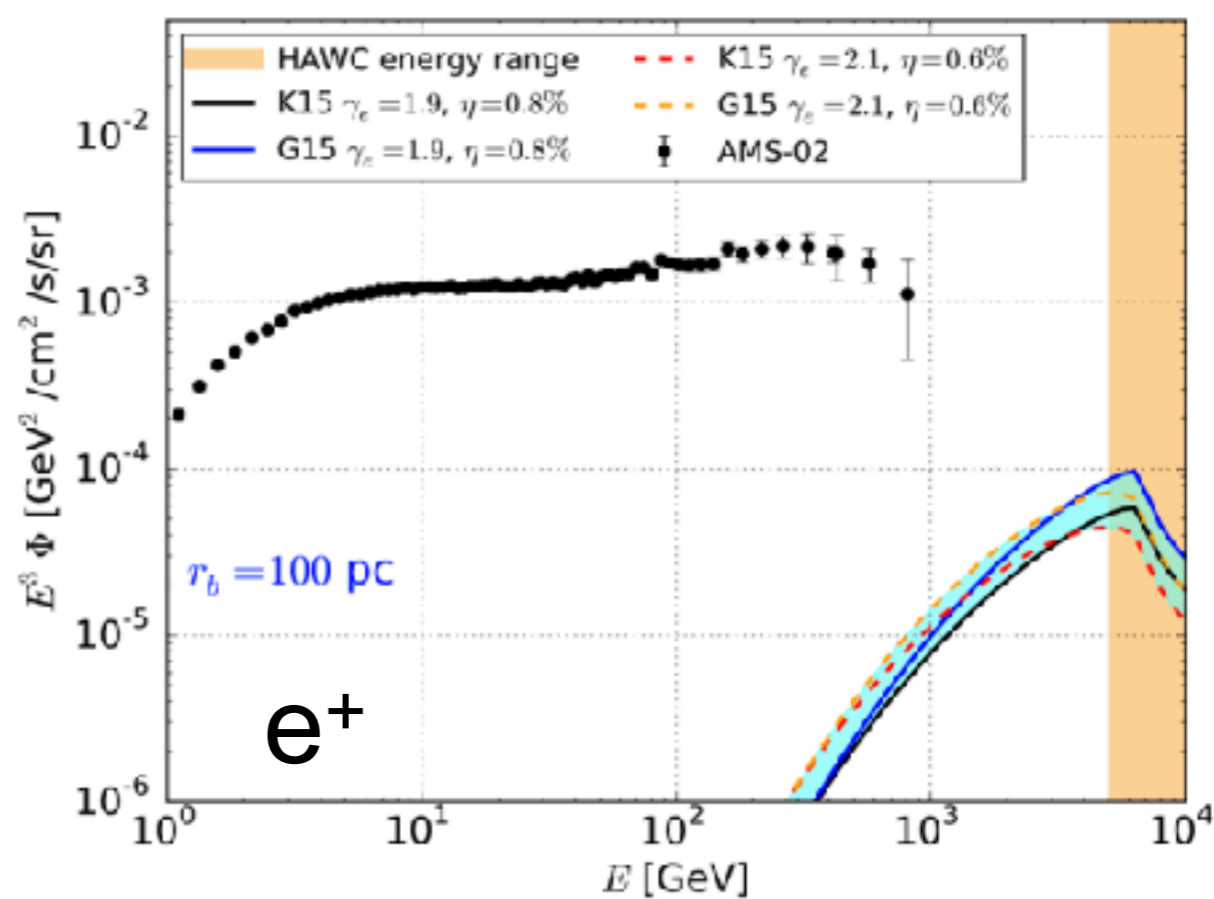
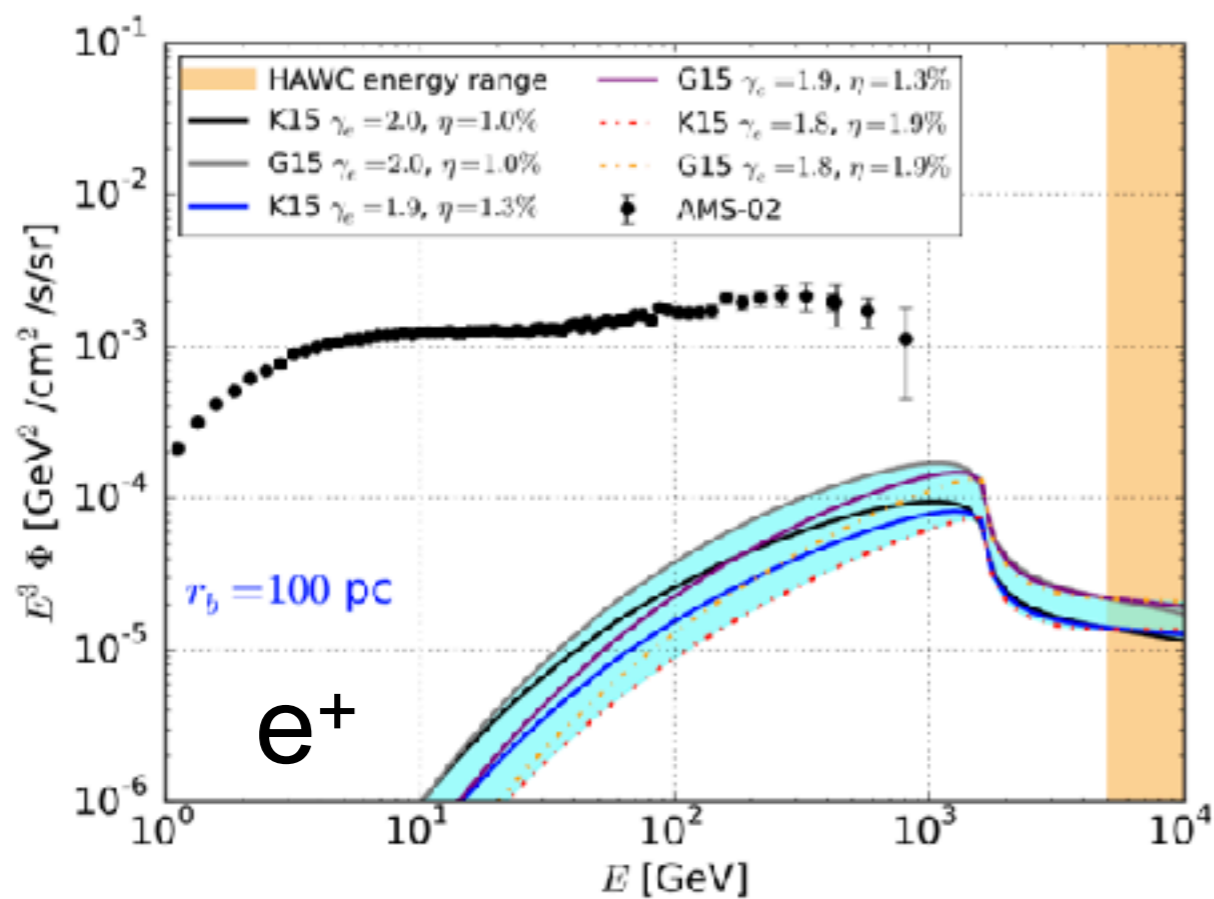
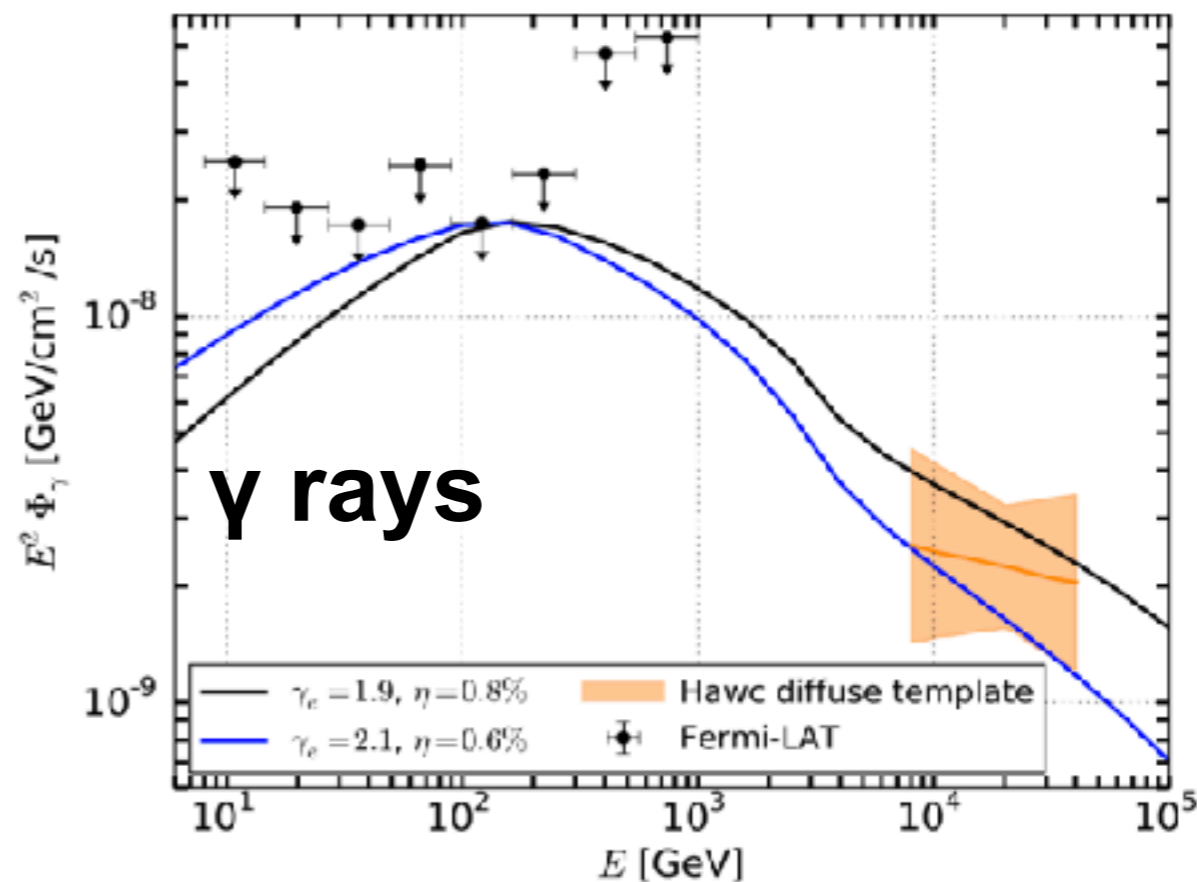
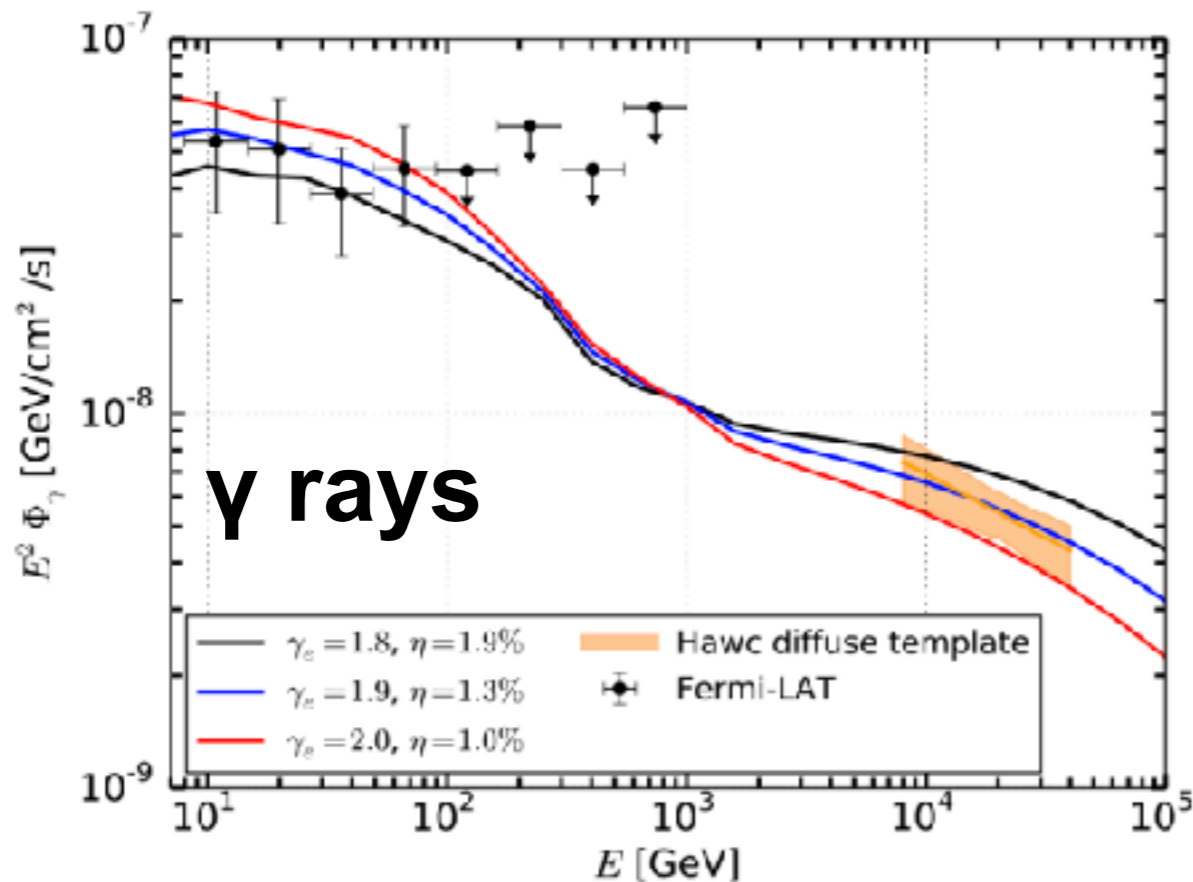
- Tuning the model with HAWC data (above 10 TeV) is not possible to have a precise prediction for the AMS-02 positron excess.
- We should use γ -ray data between 10 GeV to 1 TeV.
- *Fermi-LAT* is ideal for this scope:
 - It detects γ rays between 100 MeV to TeV.
 - It covers the entire sky every 3 hours
 - It is observing the sky since more than 10 years.

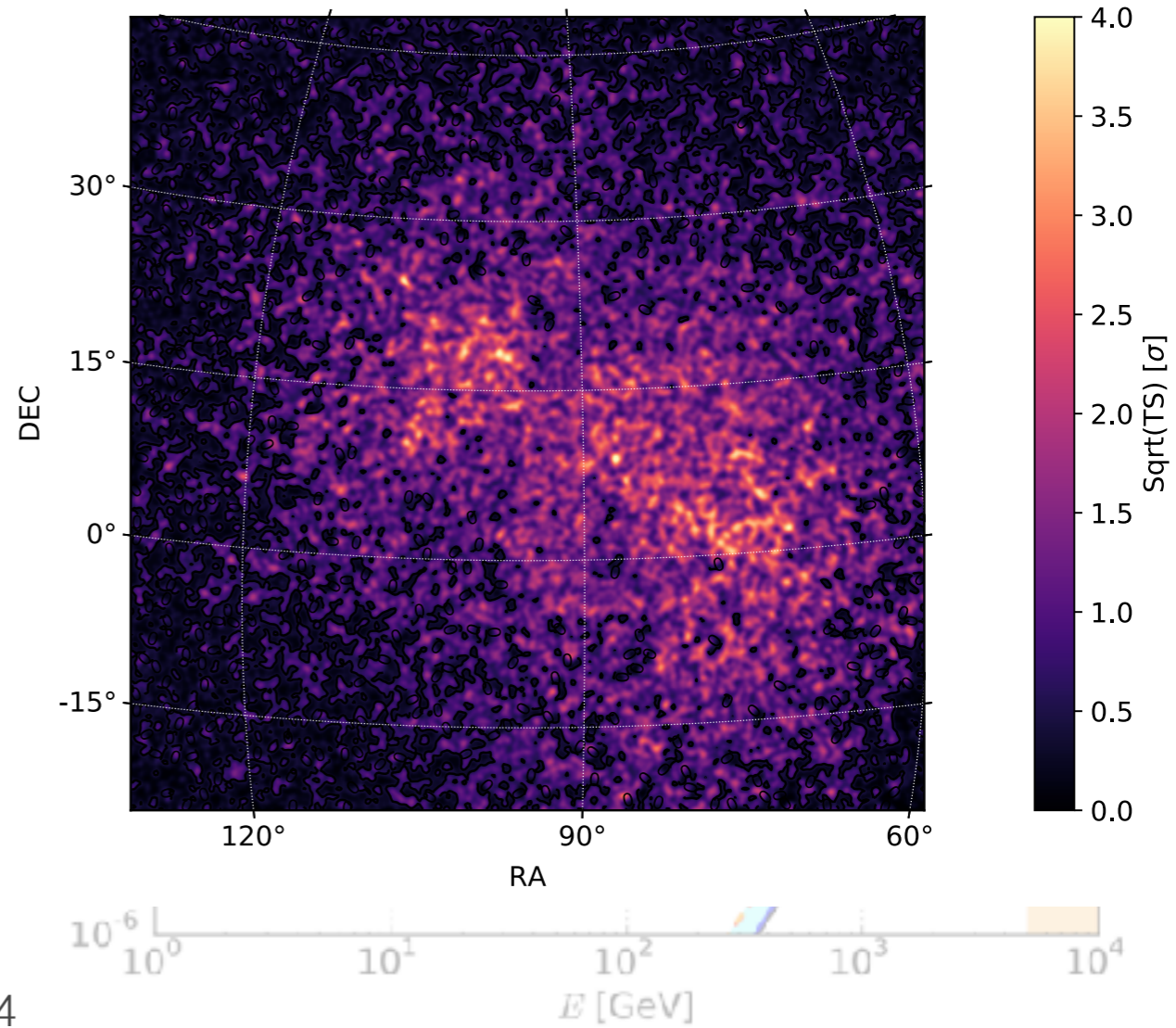
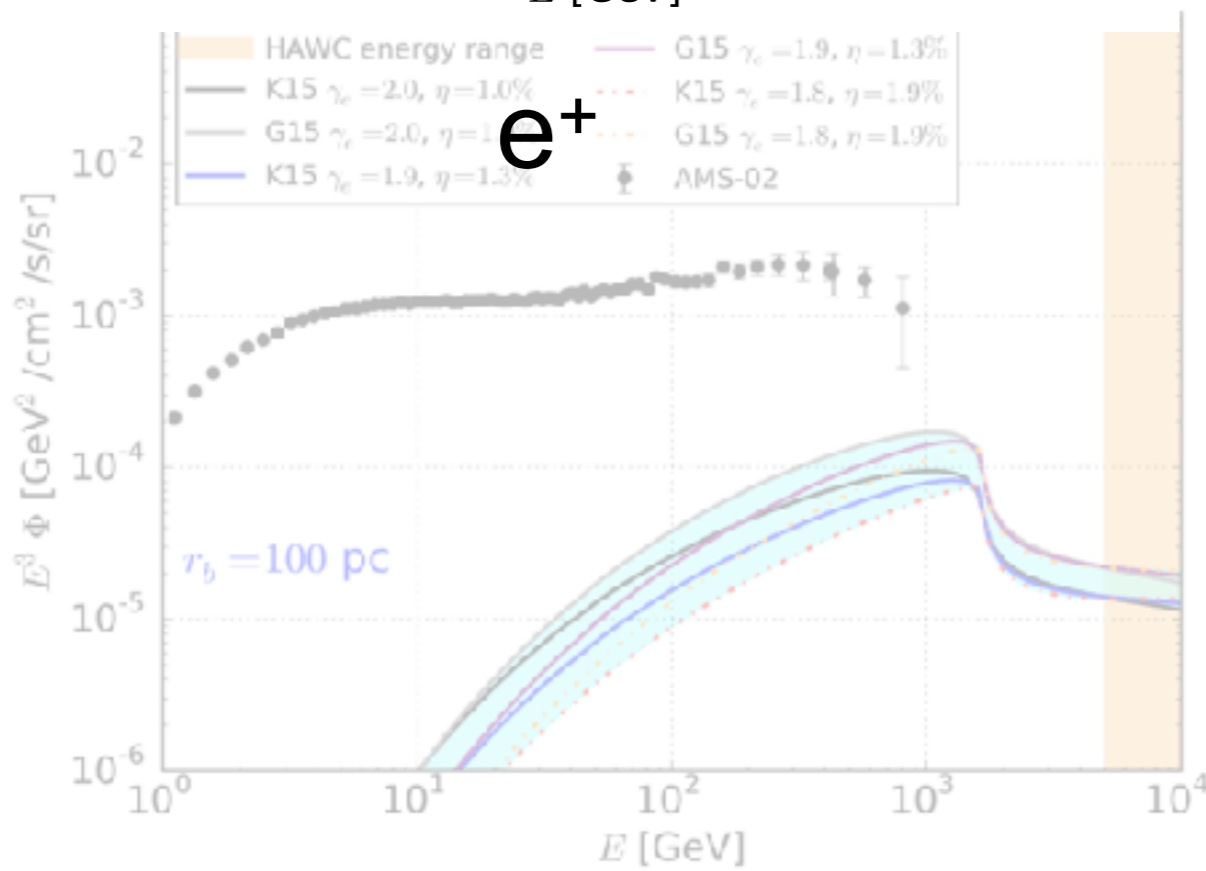
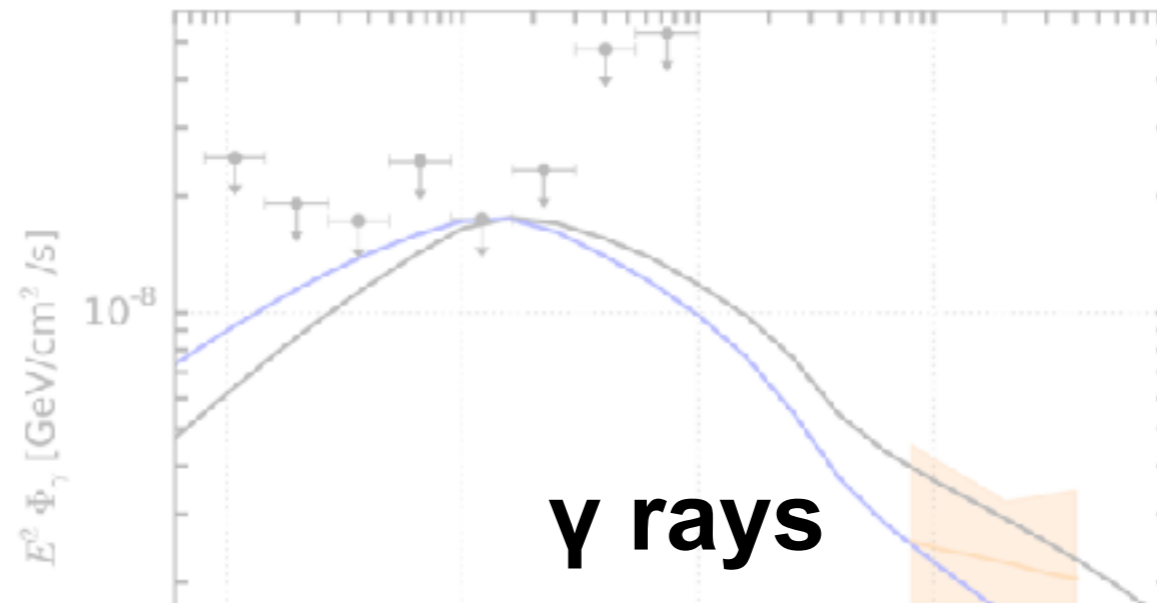
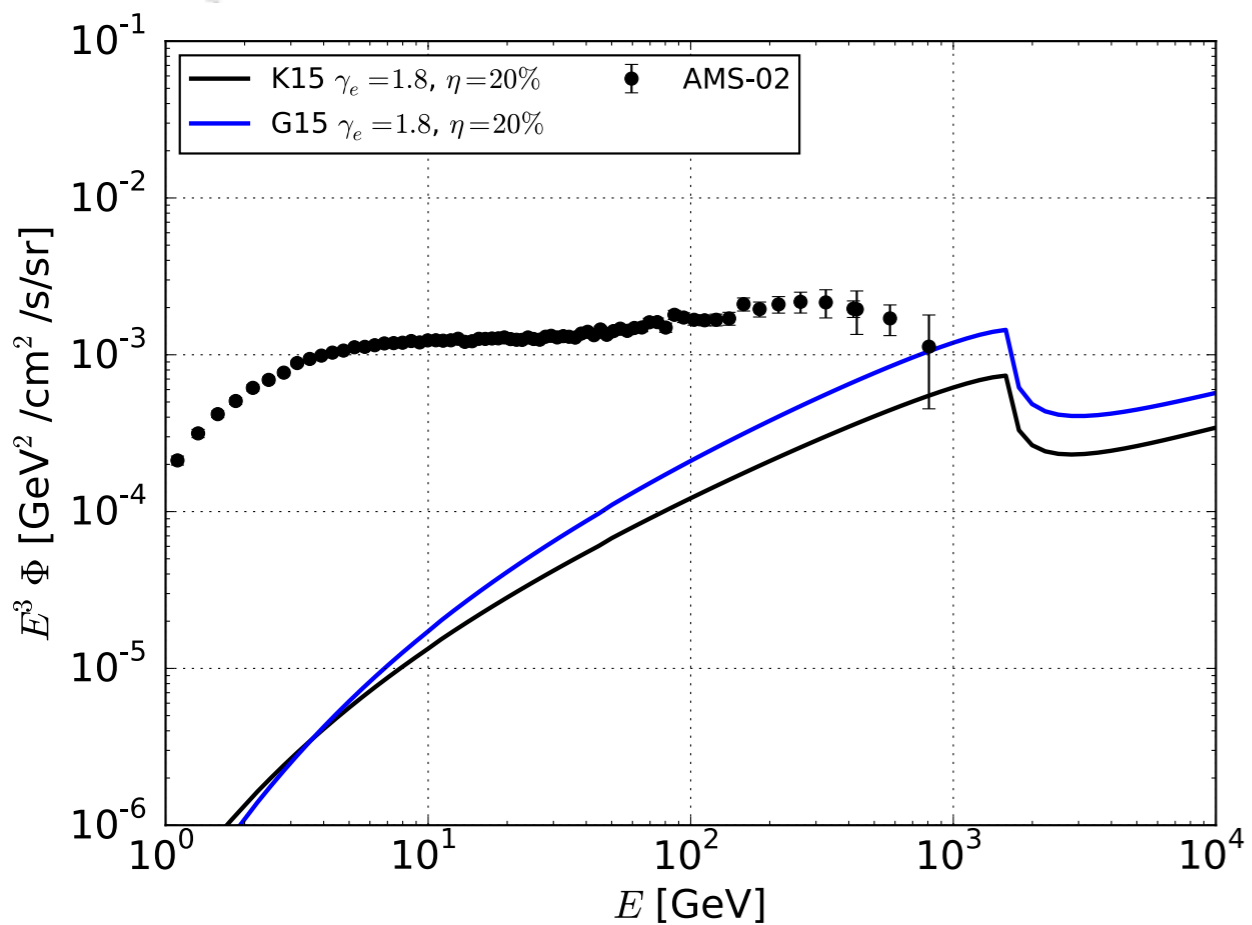


Analysis of Fermi-LAT data

- We have performed an analysis of 115 months of Fermi-LAT data for $E > 8$ GeV.
- Our model with the pulsar proper motion is preferred at least at 4σ significance.
- We find a $7.8\text{-}11.8 \sigma$ significance emission from Geminga with a diffusion $D(1 \text{ GeV}) = 2.3 \cdot 10^{26} \text{ cm}^2/\text{s}$ with $\delta = 0.33$.







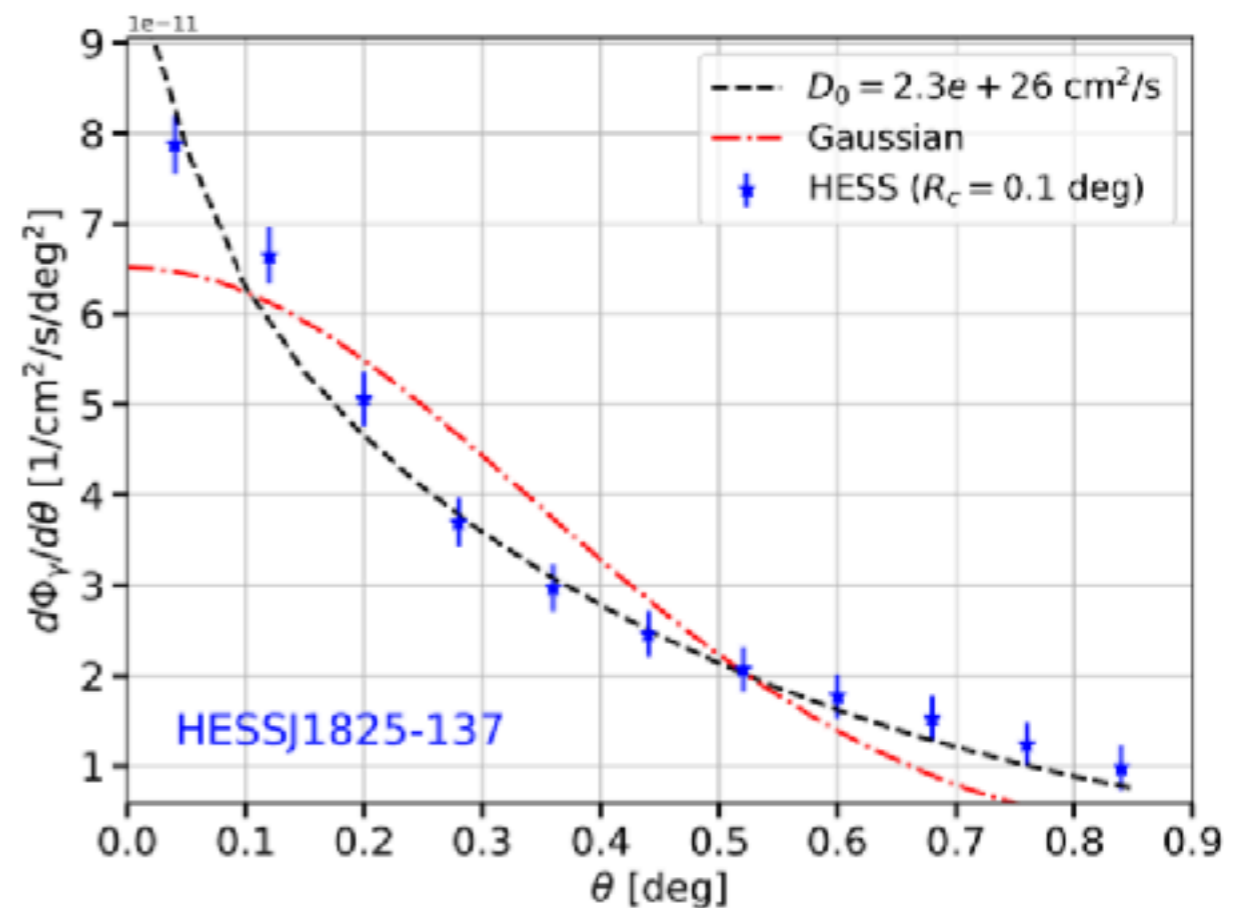
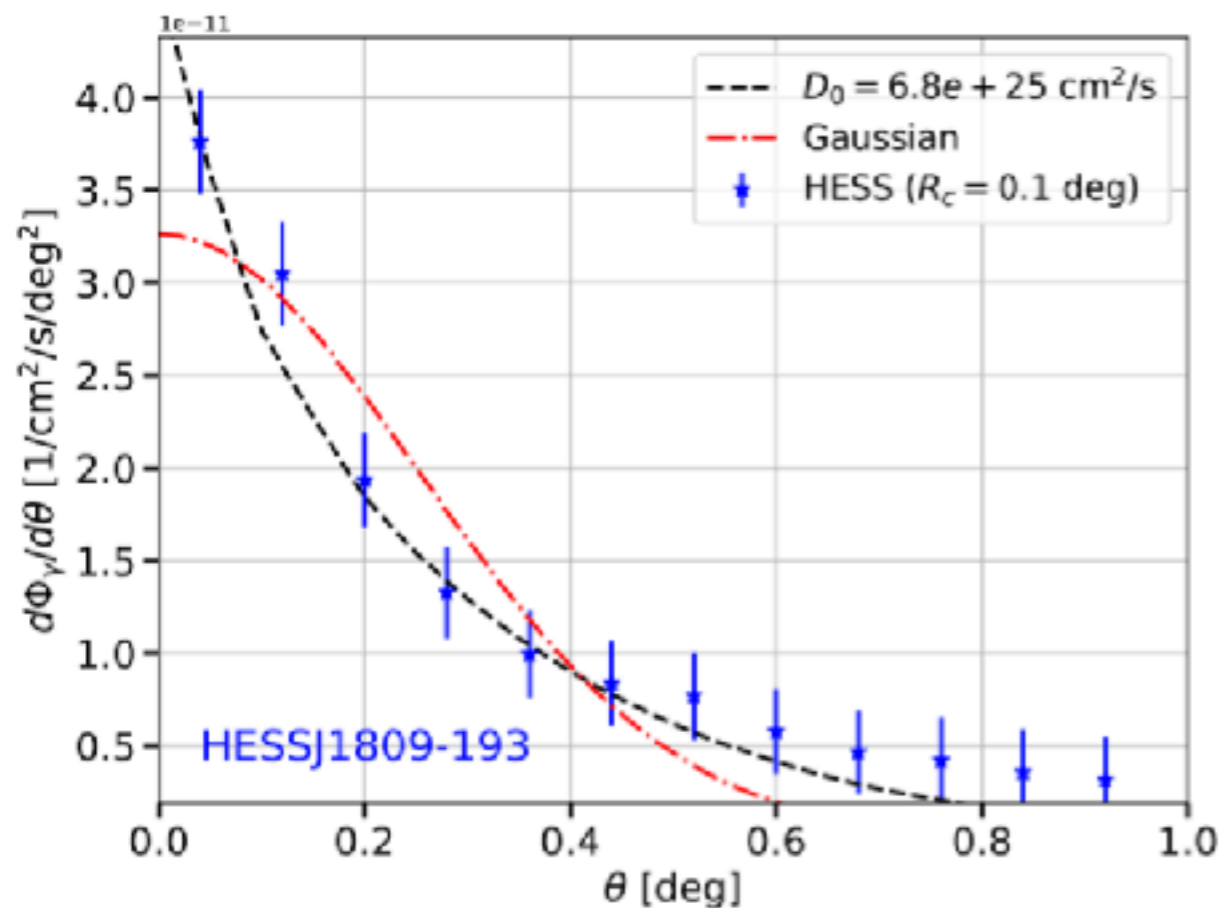
Brightest predicted halos and HAWC

- We select pulsars from the ATNF with the brightest predicted ICS halo above 1 TeV.
- Most of them are already detected by HAWC!!

PSR	l	b	d	T	\dot{E}	$\Phi_{\gamma}^{10\text{TeV}}$	θ_{es}	Name	Class
	[deg]	[deg]	[kpc]	[kyr]	[erg/s]	$[(\text{TeV cm}^2 \text{s})^{-1}]$	[deg]		
J1826-1256	18.56	-0.38	1.55	14	$3.6 \cdot 10^{36}$	$2.5 \cdot 10^{-13}$	0.89	2HWC J1825-134	UNID
J2021+3651	75.22	0.11	1.80	17	$3.4 \cdot 10^{36}$	$1.6 \cdot 10^{-13}$	0.82	2HWC J2019+367	UNID
J1813-1246	17.24	2.44	2.63	43	$6.2 \cdot 10^{36}$	$8.6 \cdot 10^{-14}$	0.60	2HWC J1812-126	UNID
J1907+0602	40.18	-0.89	2.37	20	$2.8 \cdot 10^{36}$	$6.7 \cdot 10^{-14}$	0.64	2HWC J1908+063	UNID
J0633+1746	195.13	4.27	0.19	342	$3.3 \cdot 10^{34}$	$5.8 \cdot 10^{-14}$	6.54	GEMINGA PWN	TEV HALO
B0656+14	201.11	8.26	0.29	111	$3.8 \cdot 10^{34}$	$3.4 \cdot 10^{-14}$	4.71	2HWC J0700+143	TEV HALO
B1951+32	68.77	2.82	3.00	107	$3.7 \cdot 10^{36}$	$3.0 \cdot 10^{-14}$	0.46	undetected	undetected
J1811-1925	11.18	-0.35	5.00	23	$6.4 \cdot 10^{36}$	$2.8 \cdot 10^{-14}$	0.30	2HWC J1809-190	UNID
B1823-13	18.00	-0.69	3.61	21	$2.8 \cdot 10^{36}$	$2.6 \cdot 10^{-14}$	0.41	2HWC J1825-134	UNID
J1935+2025	56.05	-0.05	4.60	21	$4.7 \cdot 10^{36}$	$2.5 \cdot 10^{-14}$	0.32	SNR G054.1+00.3	PWN
J1954+2836	65.24	0.38	1.96	69	$1.1 \cdot 10^{36}$	$2.3 \cdot 10^{-14}$	0.77	2HWC J1955+285	UNID
J1809-1917	11.09	0.08	3.27	51	$1.8 \cdot 10^{36}$	$1.5 \cdot 10^{-14}$	0.47	2HWC J1809-190	UNID
J1838-0655	25.25	-0.20	6.60	23	$5.6 \cdot 10^{36}$	$1.3 \cdot 10^{-14}$	0.22	2HWC J1837-065	PWN
J1856+0245	36.01	0.06	6.32	21	$4.6 \cdot 10^{36}$	$1.2 \cdot 10^{-14}$	0.23	2HWC J1857+027	UNID
J1958+2846	65.88	-0.35	1.95	22	$3.4 \cdot 10^{35}$	$1.2 \cdot 10^{-14}$	0.79	2HWC J1955+285	UNID
J1740+1000	34.01	20.27	1.23	114	$2.3 \cdot 10^{35}$	$1.1 \cdot 10^{-14}$	1.15	undetected	undetected
J1913+1011	44.48	-0.17	4.61	169	$2.9 \cdot 10^{36}$	$9.1 \cdot 10^{-15}$	0.27	2HWC J1912+099	SHELL
J1837-0604	25.96	0.27	4.77	34	$2.0 \cdot 10^{36}$	$8.6 \cdot 10^{-15}$	0.32	2HWC J1837-065	UNID
J1907+0631	40.52	-0.48	3.40	11	$5.3 \cdot 10^{35}$	$6.9 \cdot 10^{-15}$	0.41	2HWC J1908+063	UNID
J1928+1746	52.93	0.11	4.34	83	$1.6 \cdot 10^{36}$	$6.5 \cdot 10^{-15}$	0.30	2HWC J1928+177	UNID
J0633+0632	205.09	-0.93	1.35	59	$1.2 \cdot 10^{35}$	$5.8 \cdot 10^{-15}$	1.14	HAWC J0635+070	TEV HALO
J1831-0952	21.90	-0.13	3.68	128	$1.1 \cdot 10^{36}$	$5.6 \cdot 10^{-15}$	0.39	2HWC J1831-098	PWN
J1828-1101	20.50	0.04	4.77	77	$1.6 \cdot 10^{36}$	$5.3 \cdot 10^{-15}$	0.28	2HWC J1831-098	UNID

Is HESS detecting ICS halos?

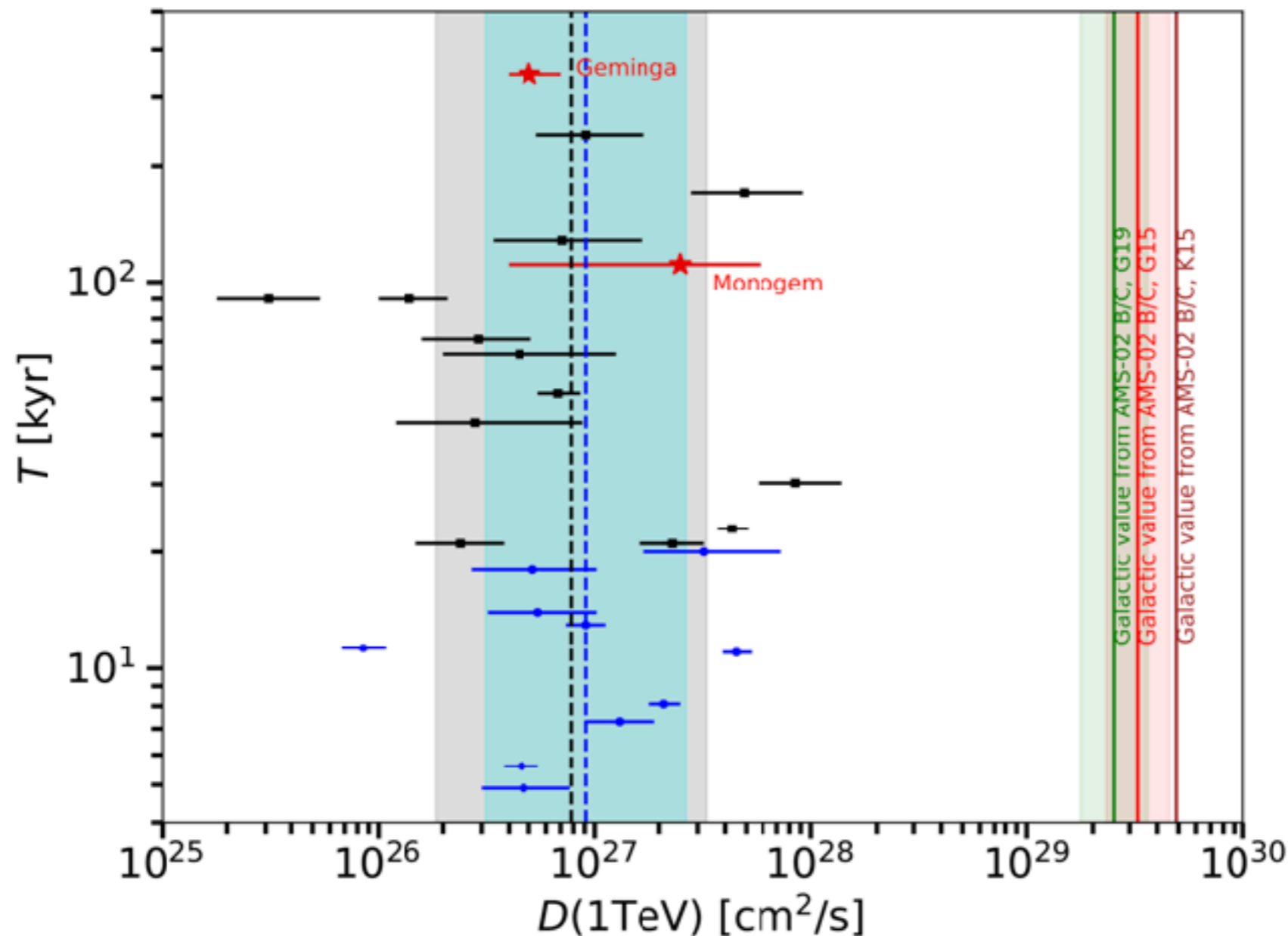
- Source detected by HESS and classified in TeVCat as PWN or Unid.
 - We have a list of 27 sources.
- We use HESS flux maps in HGPS*.
- We extract the source surface brightness that we use to calculate D_0 .



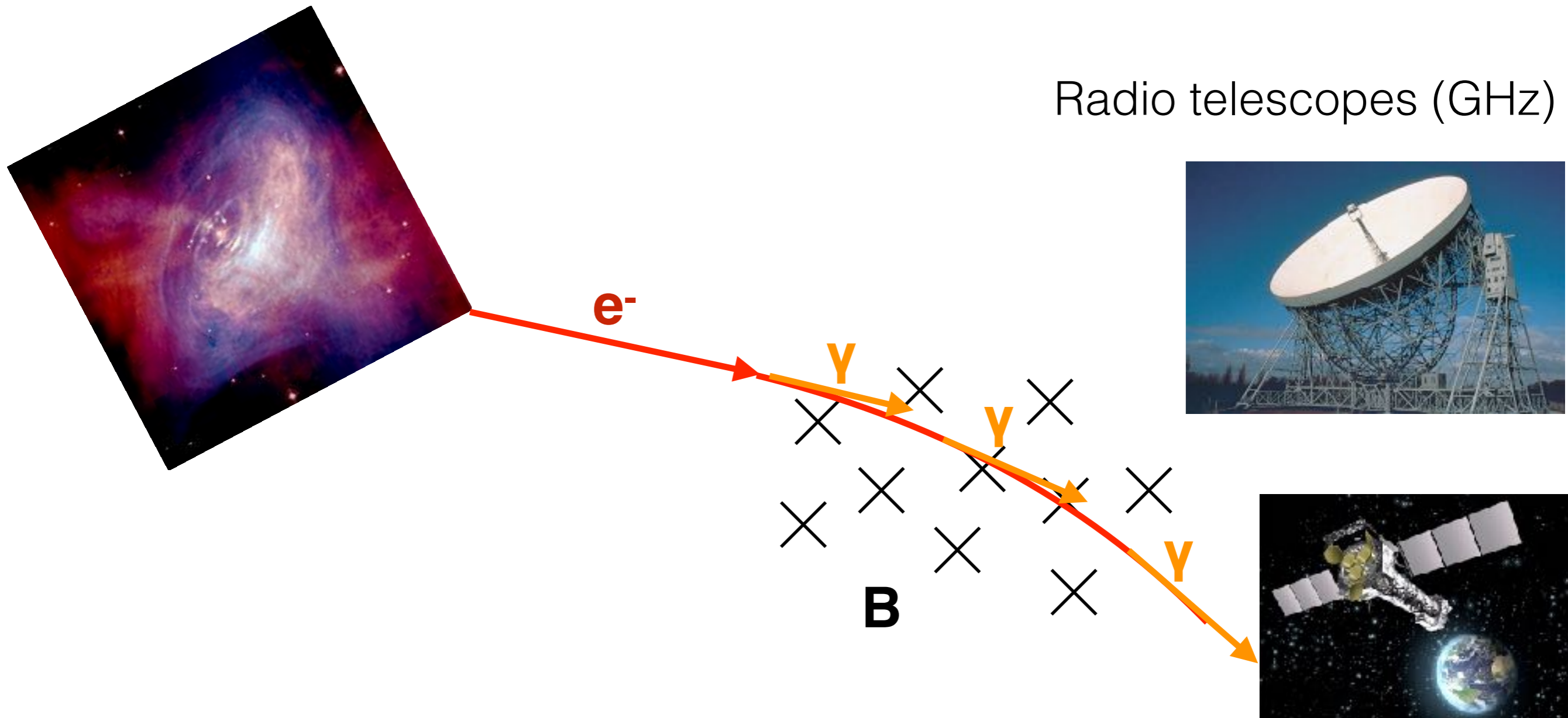
*correlation radius of 0.1 and 0.2 deg and in maps with a pixel size of 0.02 deg.

Results for the diffusion coefficient around PWNe

- We find a diffusion coefficient around the PWNe of our sample of **$8 \cdot 10^{26} \text{ cm}^2/\text{s}$ at 1 TeV**.
- The diffusion coefficient around PWNe is about 2 orders of magnitude lower than the value found from CR data.
- We find that the size of the ICS halo is on average **35 pc**.



X rays produced by synchrotron (sync) radiation



X-ray telescopes (XMM, Chandra, Swift,)

Future experiment concepts



Synchrotron halos calculation

Flux of photons for Sync.

$$\phi^{\text{IC,Sync}}(E_\gamma, \theta) = \int_{E_\gamma}^{\infty} dE \mathcal{M}(E, \theta) \mathcal{P}^{\text{IC,Sync}}(E, E_\gamma)$$

$$\mathcal{M}(E, \theta) = \int_{\Delta\Omega} d\Omega \int_0^{\infty} dr \mathcal{N}_e(E, r)$$

Synchrotron power

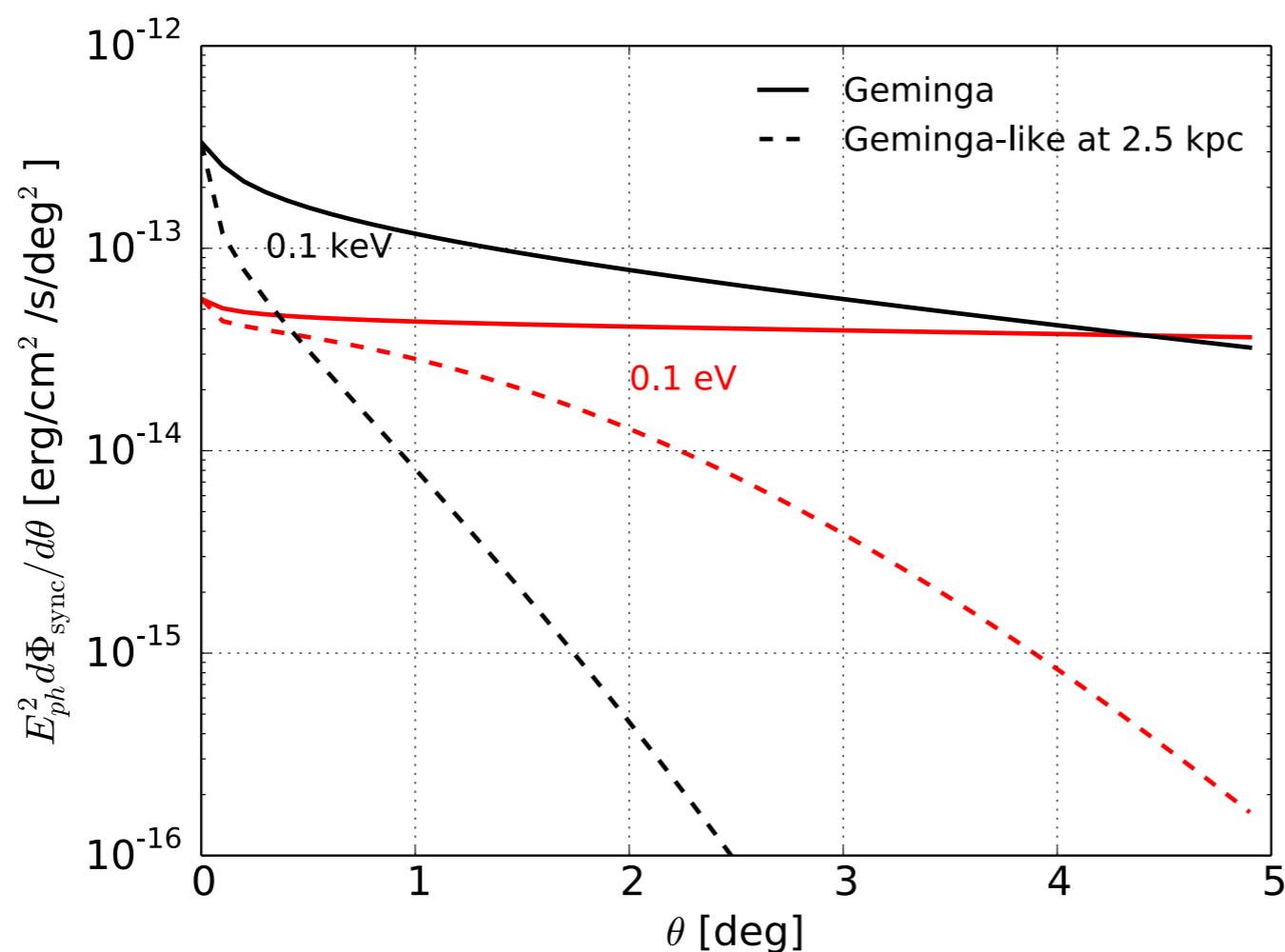
$$\frac{dN_{\text{Sync}}}{dE_\gamma dt} = \frac{1}{hE_\gamma} \frac{dE_{\text{sync}}}{d\nu dt}$$

$$\frac{dE_{\text{sync}}}{d\nu dt} = \frac{\sqrt{3}e^3 B}{m_e c^2} G(x)$$

Aharonian et al. 2010

Synchrotron flux from Geminga

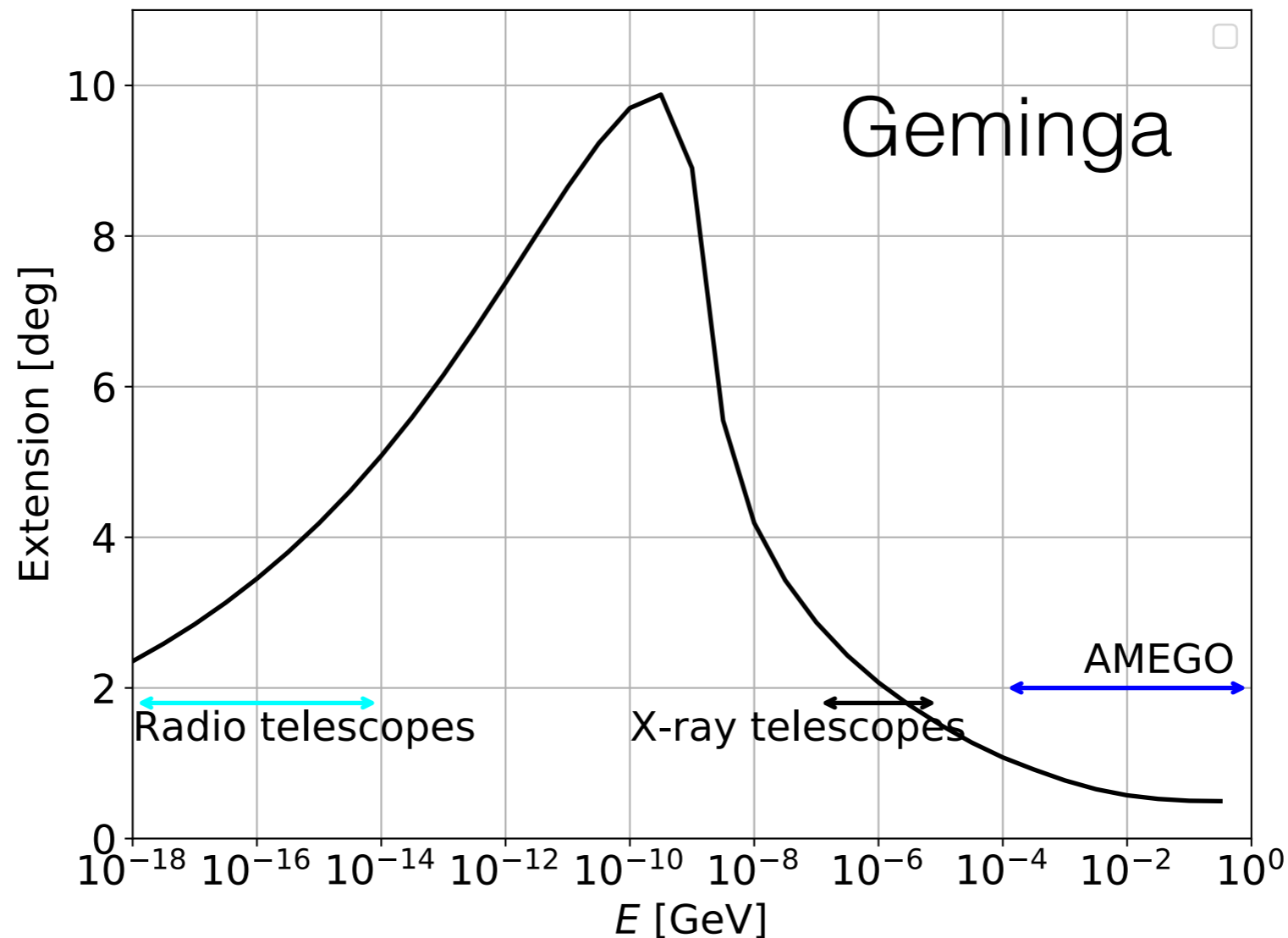
- e^\pm that produce the ICS emission at 10 TeV (10 GeV) have the peak of Sync flux at roughly 0.1 keV (0.1 eV).
- The sync halos at X-ray energies are not affected so much by proper motion.
- Surface brightness for the synchrotron emission from Geminga and a Geminga-like extended halo placed at $d = 2.5$ kpc from the Earth.



$\gamma_e = 1.8$ and $D_0 = 1.5 \cdot 10^{26}$ cm²/s and $B=3\mu\text{G}$

Extension of Geminga sync. halo

- For sources within a few kpc, sync. halos are at least of the size of one degree at radio and X-ray energies.
- This makes the detection of these halos very challenging with current X-ray and radio telescopes.

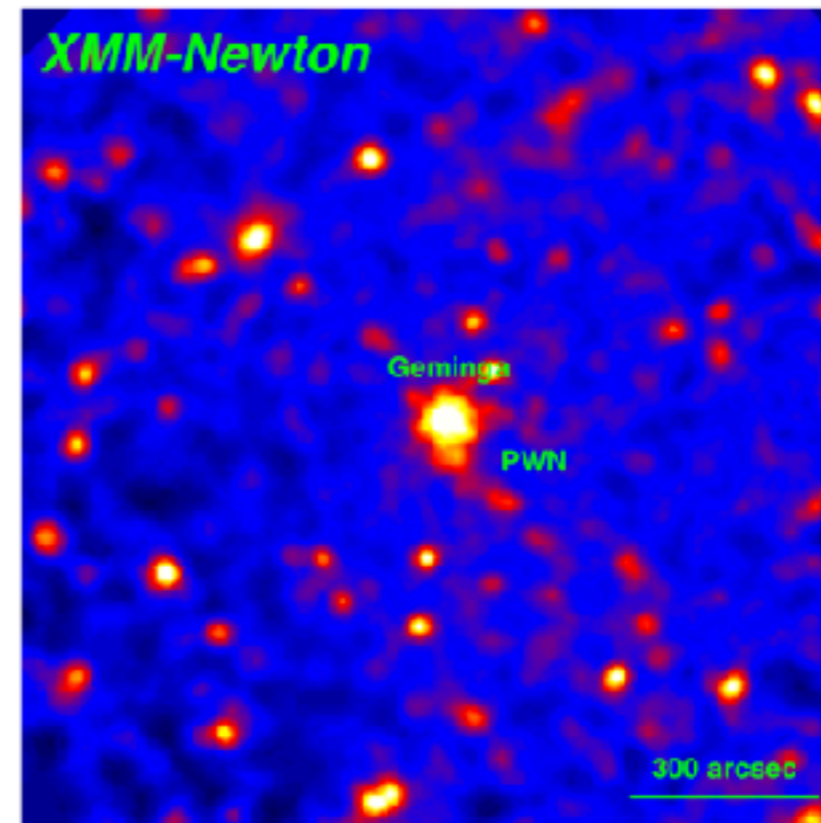
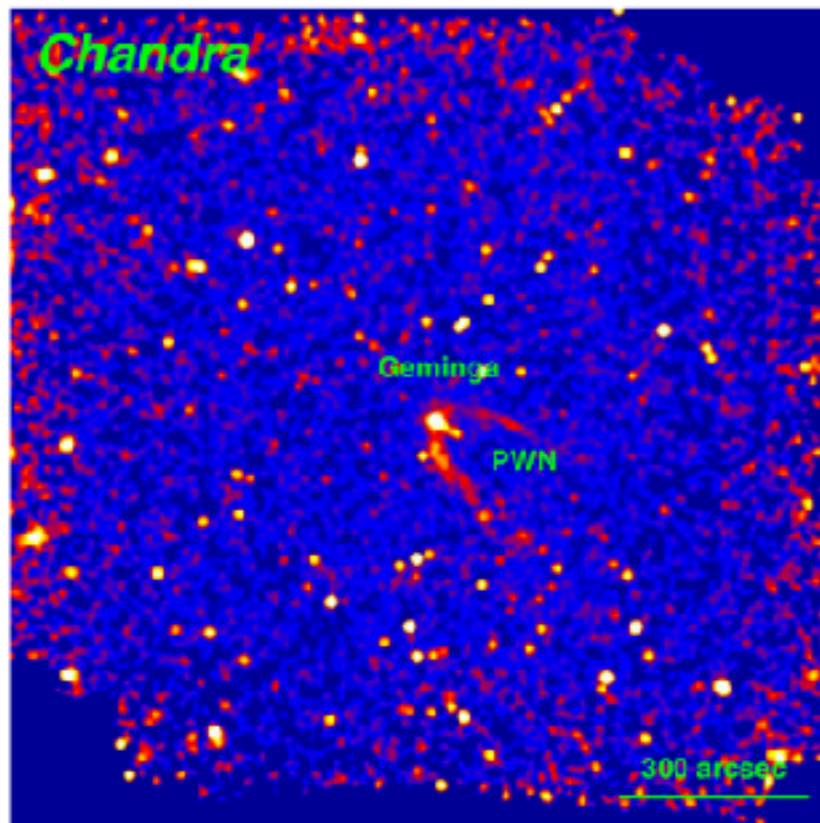
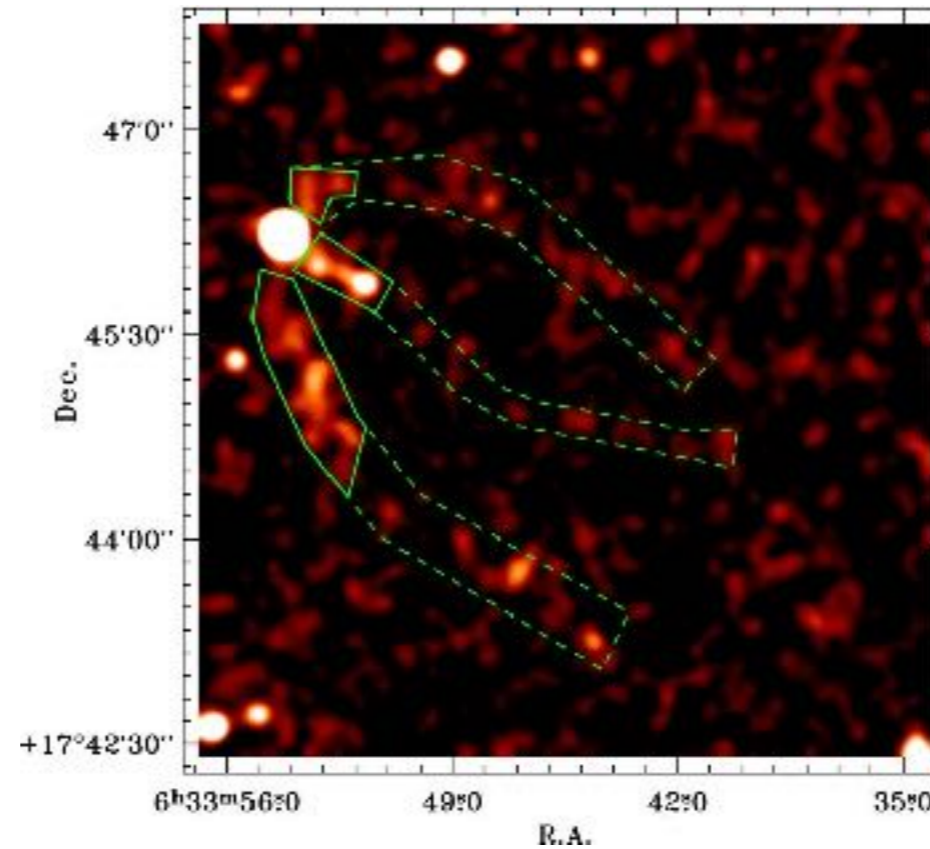


Extension of sync. halos

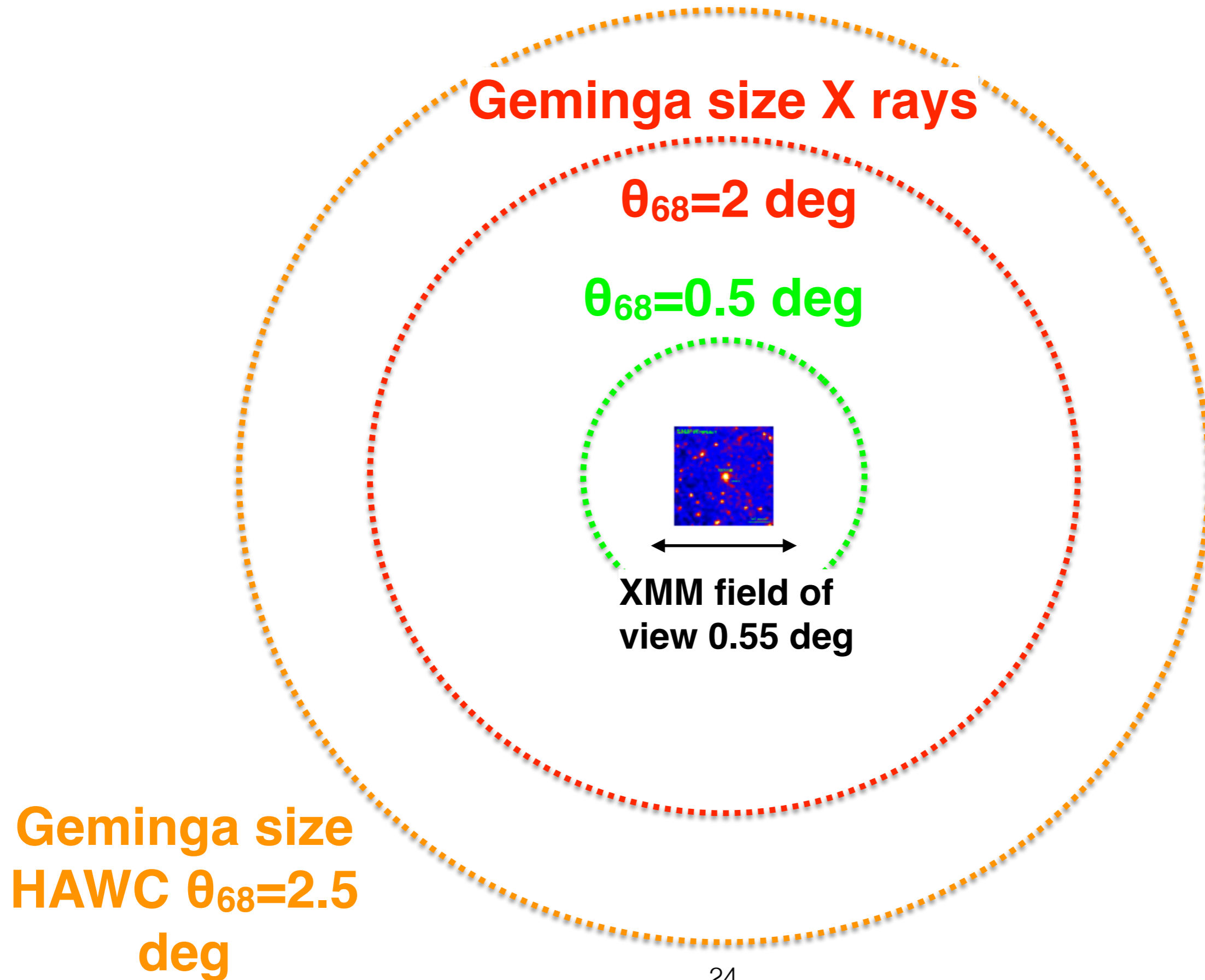
- We ranked the pulsars from the ATNF catalog according to the sync. flux in the XMM energy range.
- Most of the extensions are of the order of 0.3-0.6 deg.

Name	GLON	GLAT	d	age	Edot	θ_{68}
	[deg]	[deg]	kpc	kyr	10^{36} erg/s	[deg]
J2229+6114	106.647	2.949	3	10.5	22.5	0.45
B0833-45	263.552	-2.787	0.28	11.3	6.92	4.18
J1418-6058	313.325	0.135	1.89	10.3	4.95	0.67
J1826-1256	18.556	-0.377	1.55	14.4	3.58	0.84
J1813-1246	17.244	2.445	2.63	43.4	6.24	0.47
J2021+3651	75.222	0.111	1.8	17.2	3.38	0.72
B1706-44	343.098	-2.686	2.6	17.5	3.41	0.52
J1935+2025	56.051	-0.053	4.6	20.9	4.66	0.27
J0940-5428	277.51	-1.292	0.38	42.2	1.93	3.27
J1907+0602	40.182	-0.894	2.37	19.5	2.83	0.55
J1112-6103	291.221	-0.462	4.5	327	4.53	0.27
J1524-5625	323.0	0.351	3.38	318	3.21	0.37
J1747-2958	359.305	-0.841	2.52	25.5	2.51	0.52
B1823-13	18.001	-0.691	3.61	21.4	2.84	0.35
J1016-5857	284.079	-1.88	3.16	21	2.58	0.41
B1757-24	5.254	-0.882	3.8	15.5	2.59	0.35
B1951+32	68.765	2.823	3.0	107	3.74	0.4
B1046-58	287.425	0.577	2.9	20.3	2.01	0.45
J1105-6107	290.49	-0.846	2.36	63.3	2.48	0.52
J1803-2137	8.395	0.146	4.4	15.8	2.22	0.3
J1809-1917	11.094	0.08	3.27	51.3	1.78	0.38

Current observations of pulsars and PWNe in X rays



X-ray observations compared to halo size and HAWC data





- AMEGO, with a field of view of 2.5 sr and a spatial resolution of the order of 2 deg, is ideal to detect these halos.

Astro2020 Science White Paper

Prospects for the detection of synchrotron halos around middle-age pulsars

Multi-Messenger Astronomy and Astrophysics

Principal Author:

Name: Mattia Di Mauro

Institution: NASA Goddard Space Flight Center and Catholic University of America, Department of Physics

Email: mdimauro@slac.stanford.edu

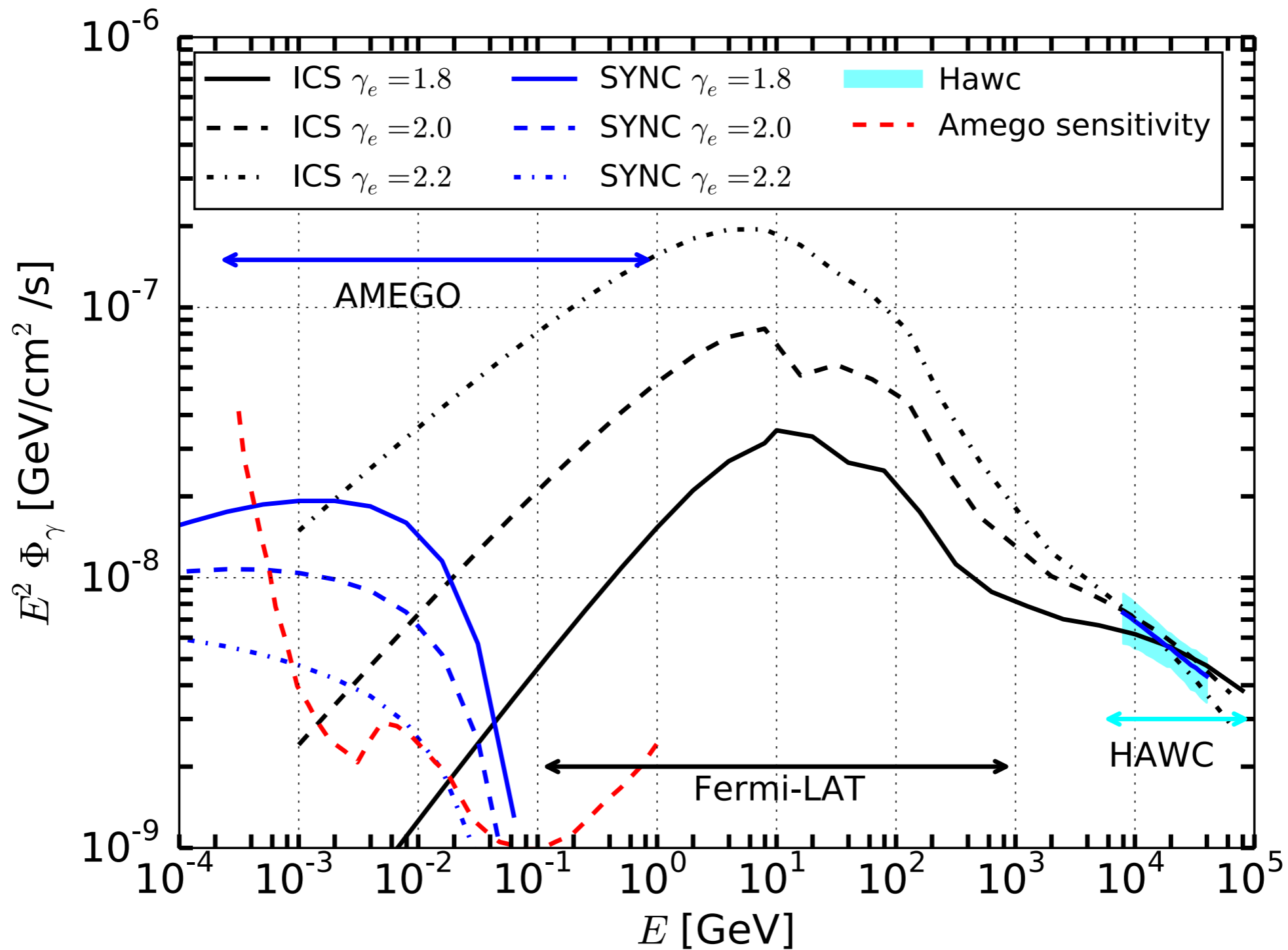
Co-authors:

Name: Manconi Silvia, Donato Fiorenza

Institution: Dipartimento di Fisica, Università degli Studi di Torino and Istituto Nazionale di Fisica Nucleare, Italy

Email: manconi@to.infn.it, donato@to.infn.it

Geminga SED from MeV to TeV



Most promising pulsars

Considering an efficiency for the conversion of energy into electrons and positrons pairs of 1% we find that **AMEGO should be able to detect about 30 synchrotron halos from middle-age pulsars.**

Name	l [deg]	b [deg]	age [kyr]	dist [kpc]	\dot{E} [erg/s]
B1055-52	285.984	6.649	535	0.09	$3.01 \cdot 10^{34}$
J0633+1746	195.134	4.266	342	0.19	$3.25 \cdot 10^{34}$
J1813-1246	17.244	2.445	43	2.63	$6.24 \cdot 10^{36}$
B1951+32	68.765	2.823	107	3.0	$3.74 \cdot 10^{36}$
J1105-6107	290.49	-0.846	63	2.36	$2.48 \cdot 10^{36}$
B0656+14	201.108	8.258	111	0.29	$3.81 \cdot 10^{34}$
B0906-49	270.266	-1.019	112	1.0	$4.92 \cdot 10^{35}$
J1809-2332	7.39	-1.995	68	0.88	$4.3 \cdot 10^{35}$
J1044-5737	286.574	1.163	40	1.9	$8.03 \cdot 10^{35}$
J1112-6103	291.221	-0.462	33	4.5	$4.53 \cdot 10^{36}$
J1459-6053	317.886	-1.791	65	1.84	$9.09 \cdot 10^{35}$
J1954+2836	65.244	0.377	69	1.96	$1.05 \cdot 10^{36}$
J1524-5625	323.0	0.351	32	3.38	$3.21 \cdot 10^{36}$
J1732-3131	356.307	1.007	111	0.64	$1.46 \cdot 10^{35}$
J1028-5819	285.065	-0.496	90	1.42	$8.32 \cdot 10^{35}$

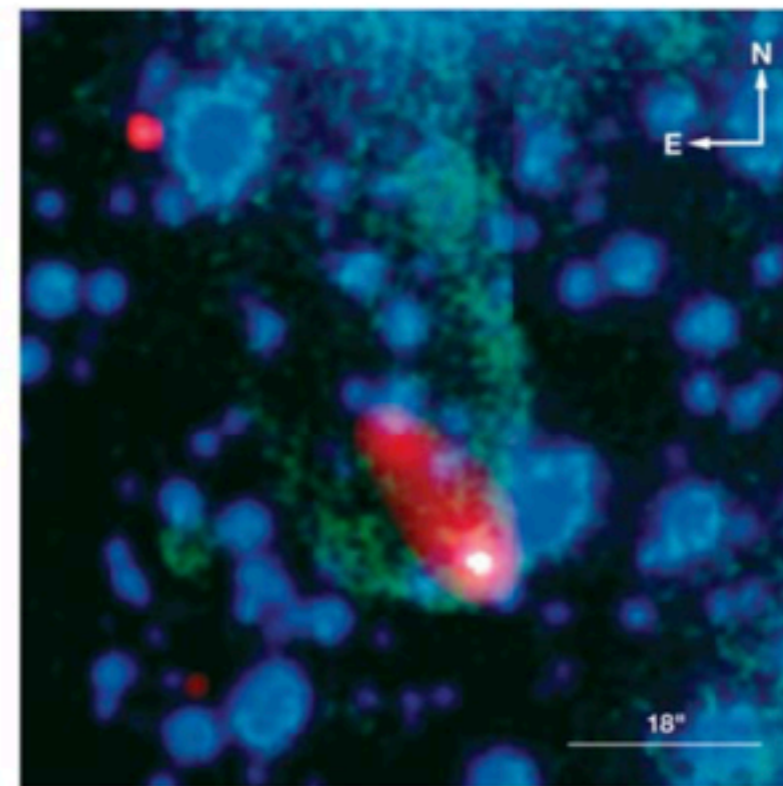
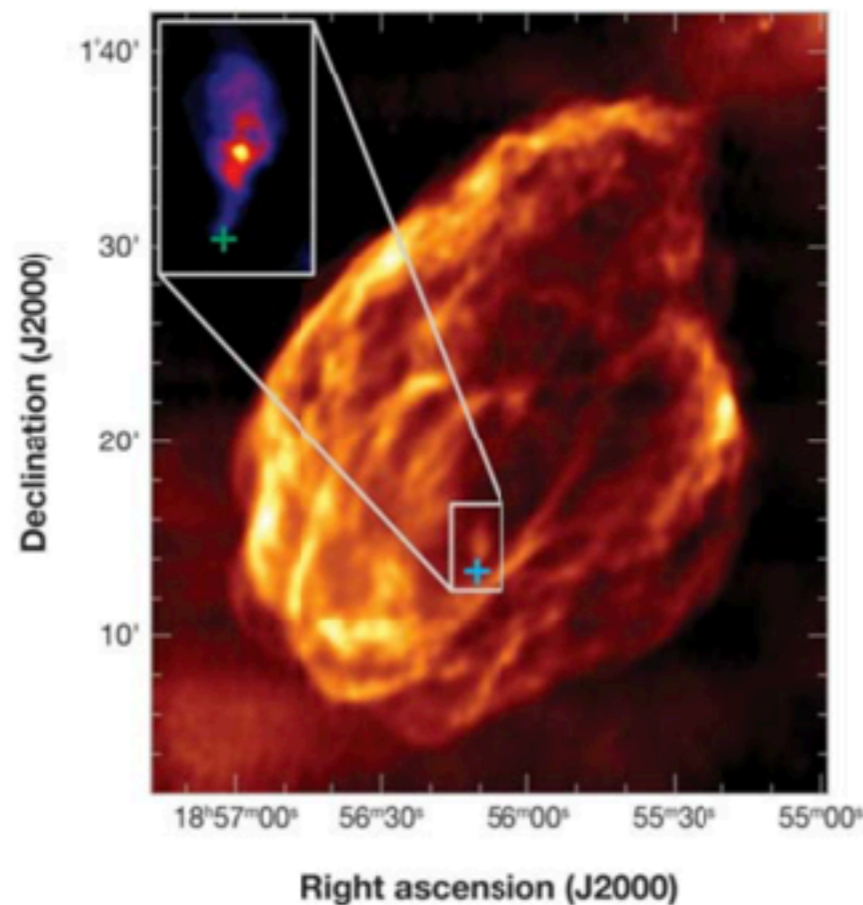
Conclusions

- Several ICS halos have been already detected at TeV energies by IACTs and HAWC.
- The first ICS halo has been detected also at GeV energies.
 - We showed the limitations of detecting halos at GeV and TeV energies.
- At lower energies Sync halos are challenging to find due to their size that is much larger or comparable with X-ray telescopes field of view.
- The future AMEGO experiment is designed to have a large field of view.
 - AMEGO could detect tens of these halos produced by Synchrotron radiation.
 - **AMEGO could thus provide key information to estimate the contribution of PWNe to the positron excess.**

Backup slide

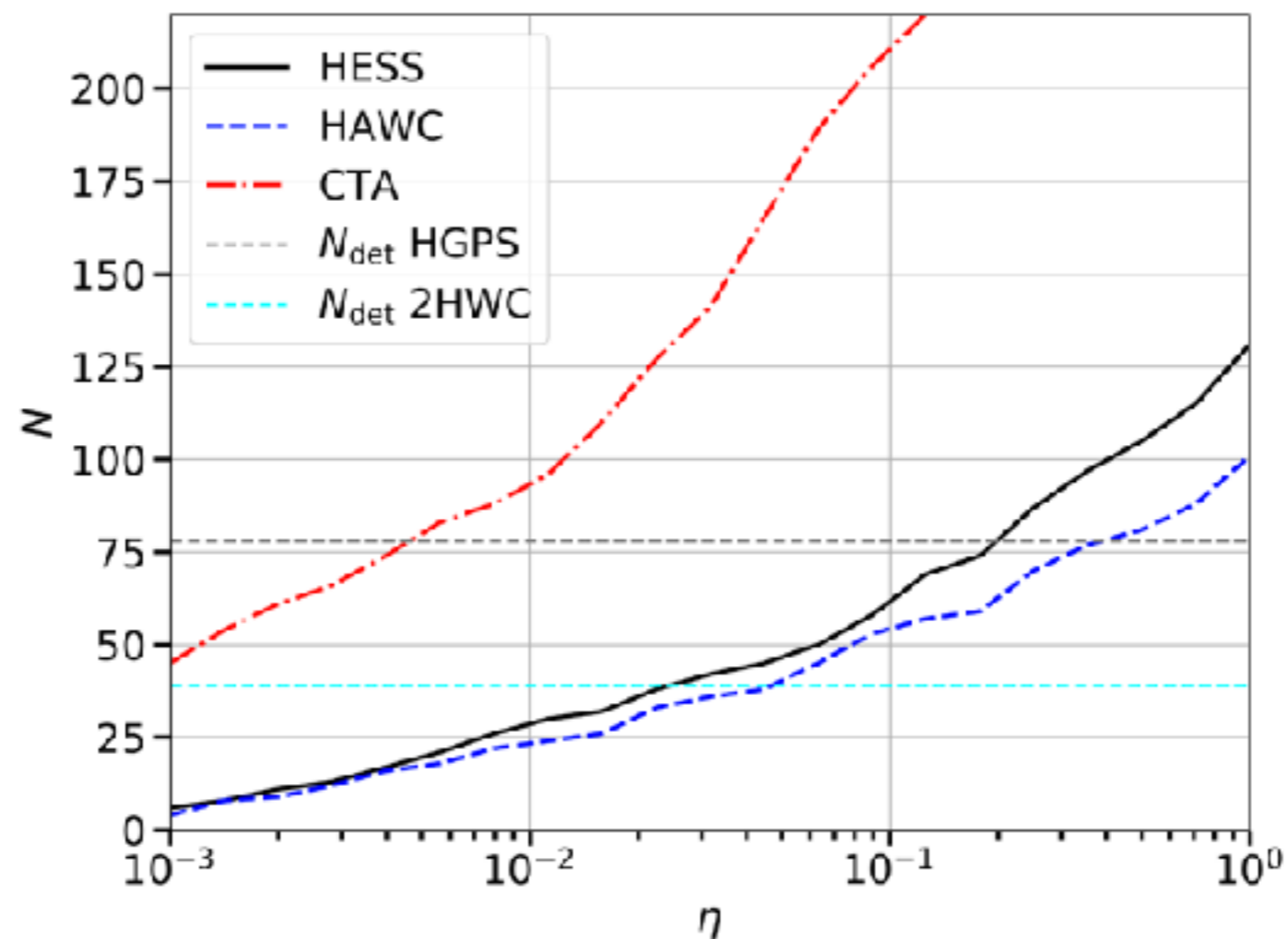
Cosmic-ray e^\pm accelerated by PWNe

- The engine of a PWN is a pulsar, i.e. a rapidly spinning neutral star (NS).
- A NS has huge magnetic fields (10^9 - 10^{12} G) which produce wind of particles extracted from the NS surface.
- This wind shines from radio to gamma rays and after a few kyrs interact with the SNR reverse shock.
- The pulsar proper motion and the interaction with the SNR reverse shock generate a relic PWN and a bow shock.



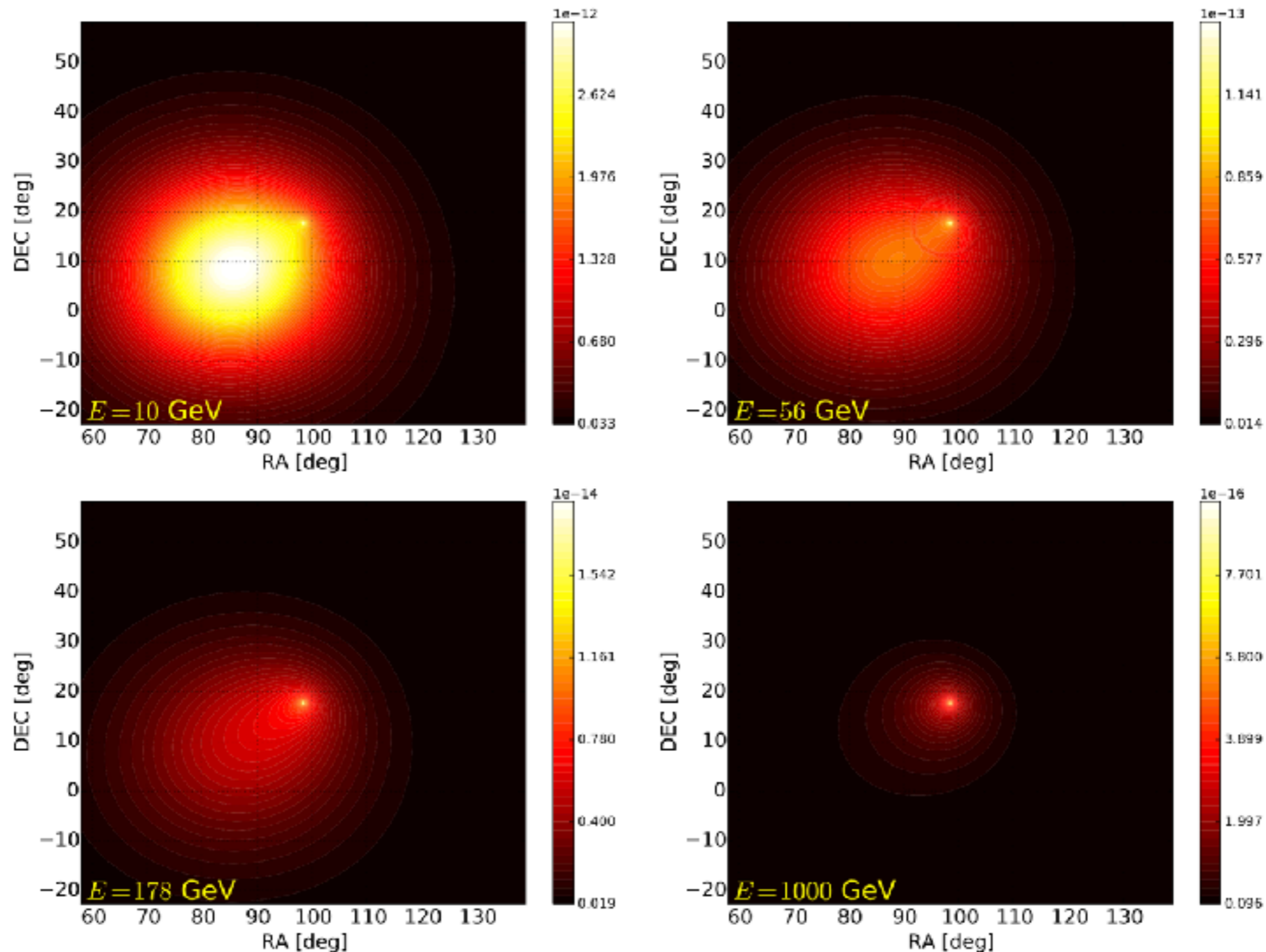
Number of detectable ICS halos

- An other interesting question is: how many ICS halos current and future gamma-ray experiments could detect?
- We took the pulsars in the ATNF catalog and we calculate the predicted gamma-ray flux.
- We focused the results on HESS, HAWC and CTA.



Gemings pulsar proper motion

- Geminga has a proper motion of 211 km/s which implies this pulsar moves about 70 pc across its age.

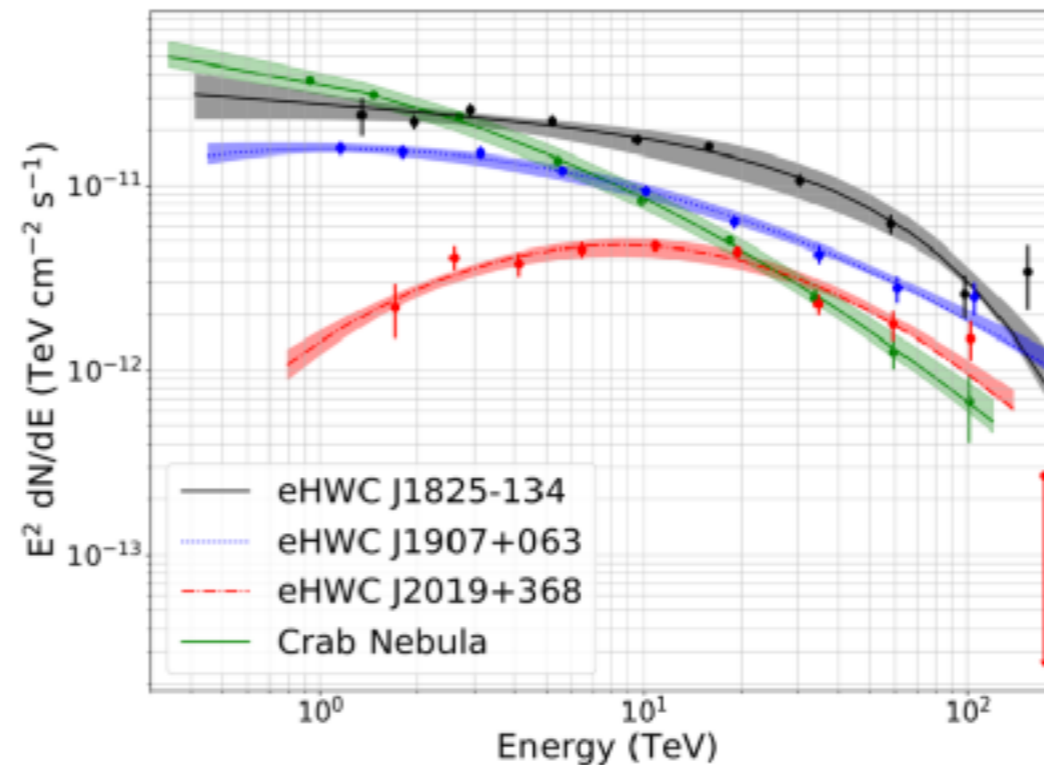


SED of three sources emitting VHE gamma rays

Source name	RA ($^{\circ}$)	Dec ($^{\circ}$)	Extension $>$ 56 TeV ($^{\circ}$)	F (10^{-14} ph cm $^{-2}$ s $^{-1}$)	$\sqrt{TS} >$ 56 TeV	nearest 2HWC source	Distance to 2HWC source($^{\circ}$)	$\sqrt{TS} >$ 100 TeV
eHWC J0534+220	83.61 ± 0.02	22.00 ± 0.03	PS	1.2 ± 0.2	12.0	J0534+220	0.02	4.44
eHWC J1809-193	272.46 ± 0.13	-19.34 ± 0.14	0.34 ± 0.13	$2.4_{-0.5}^{+0.6}$	6.97	J1809-190	0.30	4.82
eHWC J1825-134	276.40 ± 0.06	-13.37 ± 0.06	0.36 ± 0.05	4.6 ± 0.5	14.5	J1825-134	0.07	7.33
eHWC J1839-057	279.77 ± 0.12	-5.71 ± 0.10	0.34 ± 0.08	1.5 ± 0.3	7.03	J1839-065	0.96	3.06
eHWC J1842-035	280.72 ± 0.15	-3.51 ± 0.11	0.39 ± 0.09	1.5 ± 0.3	6.63	J1844-032	0.44	2.70
eHWC J1850+001	282.59 ± 0.21	0.14 ± 0.12	0.37 ± 0.16	$1.1_{-0.2}^{+0.3}$	5.31	J1849+001	0.20	3.04
eHWC J1907+063	286.91 ± 0.10	6.32 ± 0.09	0.52 ± 0.09	2.8 ± 0.4	10.4	J1908+063	0.16	7.30
eHWC J2019+368	304.95 ± 0.07	36.78 ± 0.04	0.20 ± 0.05	$1.6_{-0.2}^{+0.3}$	10.2	J2019+367	0.02	4.85
eHWC J2030+412	307.74 ± 0.09	41.23 ± 0.07	0.18 ± 0.06	0.9 ± 0.2	6.43	J2031+415	0.34	3.07

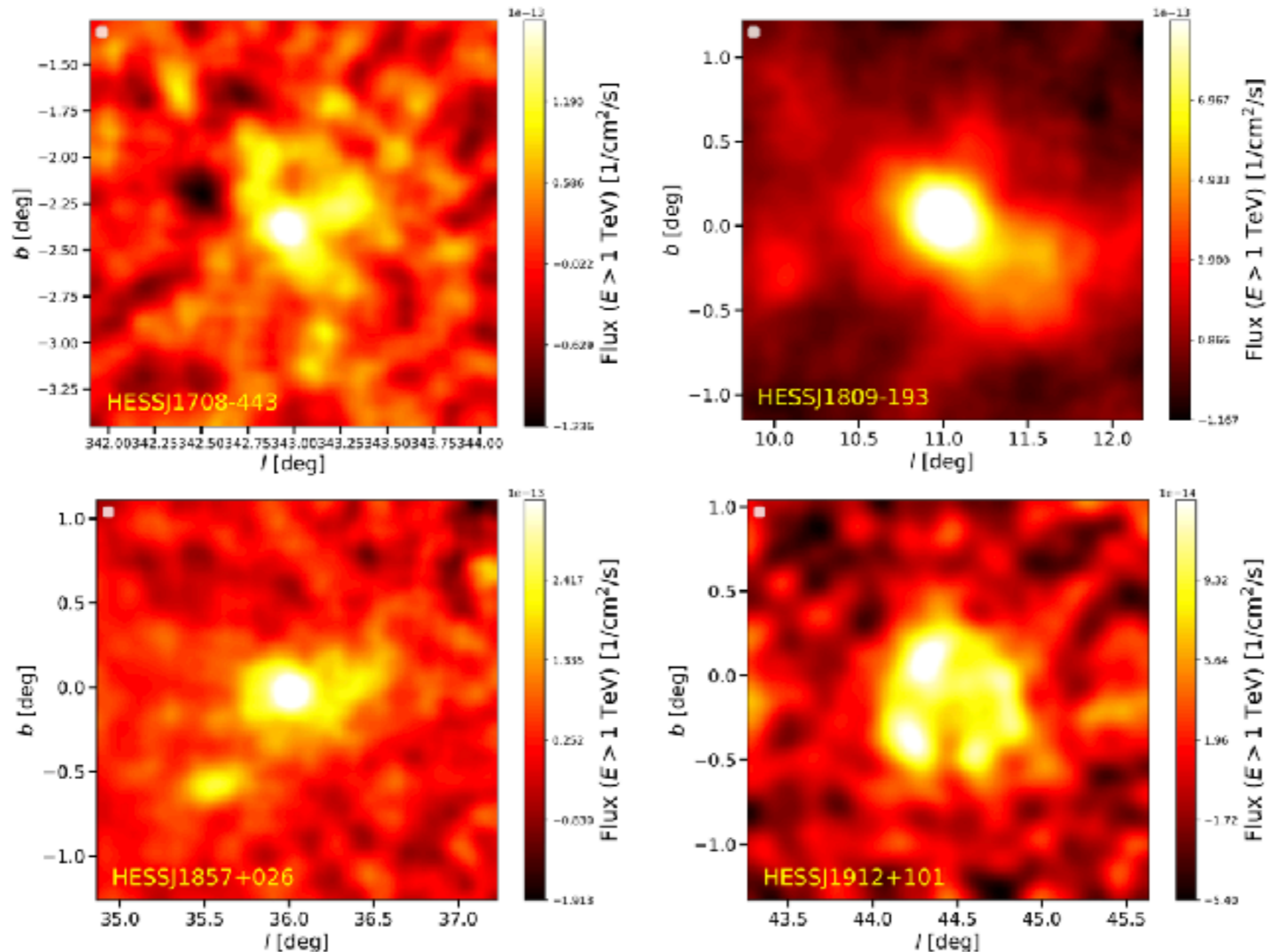
Source	\sqrt{TS}	Extension ($^{\circ}$)	ϕ_0 (10^{-13} TeV cm 2 s) $^{-1}$	α	E_{cut} (TeV)	PL diff
eHWC J1825-134	41.1	0.53 ± 0.02	2.12 ± 0.15	2.12 ± 0.06	61 ± 12	7.4

Source	\sqrt{TS}	Extension ($^{\circ}$)	ϕ_0 (10^{-13} TeV cm 2 s) $^{-1}$	α	β	PL diff
eHWC J1907+063	37.8	0.67 ± 0.03	0.95 ± 0.05	2.46 ± 0.03	0.11 ± 0.02	6.0
eHWC J2019+368	32.2	0.30 ± 0.02	0.45 ± 0.03	2.08 ± 0.06	0.26 ± 0.05	8.2



HESS flux maps

- We selected sources detected mainly by HESS because they released flux maps.
- The flux is provided for a correlation radius of 0.1 and 0.2 deg and in maps with a pixel size of 0.02 deg.
- We removed sources close to our sources of interests.



Surface brightness data

